NASA Contractor Report 3549
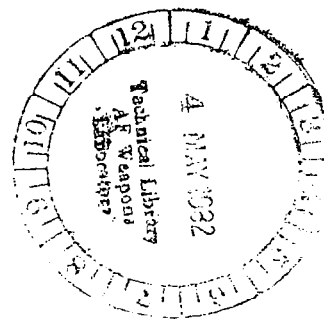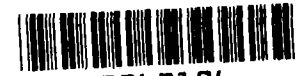
Nonlinear Theory of Shocked Sound Propagation in a Nearly Choked Duct Flow

M. K. Myers and A. J. Callegari

NASA

NASA Contractor Report 3549

Nonlinear Theory of Shocked Sound Propagation in a Nearly Choked Duct Flow

M. K. Myers
The George Washington University
Joint Institute for Advancement of Flight Sciences
Hampton, Virginia

A. J. Callegari
Advanced Analytical Research, Inc.
Princeton, New Jersey

NASA

National Aeronautics
and Space Administration

Scientific and Technical
Information Branch

1982

TABLE OF CONTENTS

SUMMARY

The development of shocks in the sound field propagating
through a nearly choked duct flow is analyzed by extending the
quasi-one dimensional nonlinear theory previously derived by the
authors. The theory is applied to the case in which sound is in-
troduced into the flow by an acoustic source located in the vicin-
ity of a near-sonic throat. Analytical solutions for the field
are obtained which illustrate the essential features of the non-
linear interaction between sound and flow.

Numerical results are presented covering ranges of variation
of source strength, throat Mach number, and frequency. It is
found that the development of shocks leads to appreciable attenua-
tion of acoustic power transmitted upstream through the near-sonic
flow. It is possible, for example, that the power loss in the
fundamental harmonic can be as much as 90% of that introduced at
the source.

1. INTRODUCTION

The possibility of reducing noise transmitted upstream in engine inlets by using a nearly choked mean flow has been recognized for some time. In a sequence of papers (refs. 1-6), the present authors have developed a nonlinear quasi-one dimensional theory of sound propagation through a high-subsonic throat which is aimed at understanding the physical mechanisms responsible for the noise reduction. The theory is derived using the method of matched asymptotic expansions. With the exception of the work reported in reference 6, the theory has thus far been applied to cases in which shock waves do not occur. It is clear, however, that it offers a possible explanation for a reduction in upstream travelling sound. A near-sonic steady flow near the throat causes a transonic trapping of waves propagating upstream, and the resulting intensification of the field gives rise to nonlinear interactions between the sound and the flow. As a result, for example, sound energy introduced by a harmonic source is partitioned into an infinite number of superharmonic components and a steady streaming component after passing through the near-sonic flow region. Even in the absence of any actual dissipation of energy, the energy transmitted out of the throat region in the fundamental harmonic can be reduced significantly compared to that imparted at the source.

Previous work by other authors which relates to the present investigation has been discussed in references 1-6. No attempt will be made here to survey all of these sources again. However, it should be noted that a fully numerical investigation of the nonlinear quasi-one dimensional problem has been carried out by Nayfeh and his co-workers (see refs. 7,8). Their numerical results confirm the existence of all of the nonlinear effects mentioned above in the shock-free case.

By far the most significant physical consequence of the nonlinearity, however, is the fact that sufficiently high source strengths or frequencies cause the nonlinear acoustic field to develop shock waves in the near-sonic flow region which ultimately appear in the sound field away from the throat region as simple acoustic discontinuities in each period of the sound wave. In earlier work (refs. 1-5) this effect was recognized, and the conditions under which shocks occur were derived. It is the purpose of the current report to carry out the necessary generalization of the theory to account for these shock waves. As will be seen, this involves an extensive nonlinear analysis which shows that complicated shock motions can occur in the throat region. The shocks are associated with two related physical effects on the sound field. First, they actually dissipate sound energy through the thermoviscous effects modelled by the shock jump conditions. Second, as will be seen in detail later, sound introduced during relatively high amplitude portions of the period can interact with the flow to

produce local supersonic conditions at the source during other portions of the period. The flow can then be said to be acoustically choked: the sound signal is blocked during this portion of the period from propagating upstream. It will be seen in the following that these nonlinear effects indeed produce a significant reduction of sound transmitted out of the near-sonic flow region. At present, to the authors' knowledge, there has been no previous analytical or numerical treatment of the shocked acoustic field reported in the literature.

The analysis in the present work is concerned primarily with the situation in which sound is introduced into the flow in the vicinity of the throat of a converging-diverging duct. It is a generalization of the work which appears in reference 6. This arrangement illustrates essentially all of the nonlinear effects of a near-sonic flow on sound, and it offers the advantage over a more general case that the solution for the field can be obtained analytically. Numerical results are given as an illustration of the theory for the special case in which the sound source is located exactly at the throat of the duct.

In Chapters 3 and 4 of the report the analytical solution for the linearized acoustic field away from the throat is reviewed, and the basic nonlinear theory valid near the throat is set out in some detail. The solution to the nonlinear inner problem is developed in Chapter 5, including a detailed analysis of the shock waves which arise in the throat region. Then in Chapter 6 the shocked inner solution is asymptotically matched to the outer solution to yield a complete description of the field in terms of a set of easily evaluated integrals and the solution of two pairs of transcendental equations.

One major result of the present analysis is the development of a measure of the sound energy dissipated by shocks in the throat region of the duct. The usual concept of acoustic energy flux is not sufficient to study sound energy in this region owing to the fact that the field there is not described by linearized theory. In Chapter 7 an appropriate generalization of acoustic energy flux is introduced, and this leads to a relatively simple formula describing the sound energy dissipated by thermoviscous effects in the nonlinear theory. This dissipation process is extremely significant: typical results presented later show that as much as 40 to 50% of the total sound power introduced at the source can be lost during propagation of the sound upstream when the throat Mach number is only as high as 0.9. In combination with this dissipation, the spreading of energy among harmonics can lead to a reduction of power in the fundamental in the vicinity of 90%. It is emphasized that this almost total shutting down of sound in the first harmonic occurs even though the basic steady flow is relatively far from being choked.

4

2. SYMBOLS AND NOMENCLATURE

a	throat curvature parameter
$A(x)$	duct cross-sectional area, m^2
$A_{1n}^{\pm}, B_{1n}^{\pm}$	see equation (3.11)
A_n	magnitude of A_{1n}
c_s	stagnation sound speed, ms^{-1}
$c_0(x)$	sound speed in steady flow
c_{11}, c_{12}, d_{02}	see equation (3.12)
$C_n(x), D_n(x)$	Fourier coefficients (eq. 6.4)
$D(N)$	integration constant (eq. 5.24)
$\bar{E}, E^*, \tilde{E}, E$	dimensionless energy densities
$g(x;\varepsilon)$	see equation (6.3)
$G(x;\varepsilon)$	see equation (3.5)
$G_0(x)$	$G(x;\varepsilon=0)$
$G_{in}, i=1,\ldots,4$	see equation (3.12)
$H(x;\varepsilon)$	shock location
$H_0(X)$	leading order inner representation of $H(x;\varepsilon)$
I	time-averaged dimensionless power flow
I_{1n}, I_{2n}, J_n	see equations (6.9-6.10)
K	parameter in Crocco-Tsien Mach number distribution
L	characteristic length, m
$M(x;\varepsilon)$	steady flow Mach number
$M_0(x)$	$M(x;\varepsilon=0)$
$m_1(X)$	inner expansion Mach number term
$N, \tilde{N}$	source amplitudes
$\bar{p}(x,t;\varepsilon)$	total fluid pressure, Nm^{-2}
$p(x,t;\varepsilon)$	dimensionless perturbation pressure
$p_1(x;t;\varepsilon)$	first-order outer perturbation pressure
$p_0(x,t)$	$p_1(x,t;\varepsilon=0)$
$r_1(X,t), r_2(X,t)$	inner density expansion terms
$R(x)$	steady flow density, kgm^{-3}

t	dimensionless time
T	modified dimensionless time, $a^{\frac{1}{2}}t$
$U, \hat{U}, \breve{U}$	source velocity amplitude ms^{-1}
$\bar{u}(x,t;\varepsilon)$	total fluid velocity, ms^{-1}
$u(x;t;\varepsilon)$	dimensionless perturbation velocity
$u_1(x,t;\varepsilon)$	first order outer perturbation velocity
$u_0(x,t)$	$u_1(x,t;\varepsilon=0)$
V	shock velocity, ms^{-1}
$\bar{W}, W*, \tilde{W}, W$	dimensionless energy fluxes
W_2°	first order outer representation of W
W_n^i	inner expansion energy flux terms
x	dimensionless axial coordinate
x_0, x_e	source and exit locations
X	inner axial coordinate (eq. 4.1)
X_0	inner location of source
γ	ratio of specific heats
δ	outer acoustic disturbance level
ε	throat Mach number deviation from unity
θ_n	phase angle in inner solution
$\mu_1(X,t), \mu_2(X,t)$	inner velocity expansion terms
$\Pi(X,t)$	inner dependent variable (eq. 5.3)
$\bar{\rho}(x,t;\varepsilon)$	total fluid density kgm^{-3}
$\rho(x,t;\varepsilon)$	dimensionless perturbation density
$\rho_1(x,t;\varepsilon)$	first-order outer perturbation density
$\rho_0(x,t)$	$\rho_1(x,t;\varepsilon=0)$
$\sigma_1(X,t), \sigma_2(X,t)$	inner pressure expansion terms
τ	characteristic parameter
$\phi(T)$	source function (eq. 5.10)
ψ_n	phase angle in outer expansion (eq. 6.1)
ω	dimensionless frequency
Ω	modified frequency, $a^{-\frac{1}{2}}\omega$

Special Notation

			denotes magnitude
$< \ >$	denotes time average over one period
$[\quad]$	denotes jump across shock
subscript s	denotes stagnation value
subscript n	denotes a harmonic
superscript i	denotes inner variable
superscript $\circ$	denotes outer variable
superscript $\pm$	denotes x>0, x<0, respectively
subscript 1,2	used on $\tau, \phi(\tau), \Pi(\tau)$ to denote downstream and upstream sides of shock, respectively

3. FORMULATION AND OUTER EXPANSIONS

Perturbation Equations

Provided that the acoustic wavelength is sufficiently large and the area variation is sufficiently slow, the propagation of sound in a duct of cross-sectional area A(x) carrying an inviscid ideal gas flow can be described by the equations of quasi-one dimensional gas dynamics (ref. 9):

$$c_s \bar{\rho}_t + \bar{u}\bar{\rho}_x + \bar{\rho}\bar{u}_x + \bar{\rho}\bar{u} \, A'/A = 0,$$

$$c_s \bar{u}_t + \bar{u}\bar{u}_x + \bar{p}_x/\bar{\rho} = 0, \qquad (3.1)$$

$$c_s \bar{p}_t + \bar{u}\bar{p}_x - c^2(c_s \bar{\rho}_t + \bar{u}\bar{\rho}_x) = 0.$$

In equation (3.1) $\bar{\rho}$, $\bar{u}$, and $\bar{p}$ are the total fluid density, axial velocity, and pressure, respectively; c is the sound speed in the gas, and c_s is its stagnation value. The independent variables x and t are dimensionless, being measured in units of L and L/c_s, respectively, where L is a characteristic length associated with the axial variation in A(x). The geometry of the problem is as indicated in figure 1; the origin of x is chosen to correspond to a throat: $A'(0) = 0$.

The velocity, density, and sound speed of the basic steady flow are denoted by U(x), R(x), and c_0(x), respectively. Then the pressure in the steady flow is $c_0^2 R/\gamma$, where γ is the specific heat ratio of the gas, and U(x) and R(x) satisfy

$$UR' + RU' + RUA'/A = 0$$
$$\qquad\qquad\qquad\qquad\qquad (3.2)$$
$$UU' + c_0^2 R'/R = 0.$$

It is convenient to study unsteady perturbations about the basic steady flow in the duct in terms of dimensionless perturbation quantities ρ(x,t), u(x,t), and p(x,t) defined by

$$\bar{\rho}(x,t) = R(x)[1 + \rho(x,t)], \quad \bar{u}(x,t) = U(x)[1 + u(x,t)],$$
$$\bar{p}(x,t) = \frac{c_0^2 R}{\gamma}[1 + p(x,t)]. \qquad (3.3)$$

The usual acoustic perturbations are then given by $R(x)\rho(x,t)$, $U(x)u(x,t)$, and $c_0^2(x)R(x)\,p(x,t)/\gamma$. Substitution of equations (3.3) into equations (3.1) and employing the relations (3.2) yields the system of equations on ρ, u, and p in the form

$$G^{\frac{1}{2}}\rho_t + M\{(1+u)\rho_x + (1+\rho)u_x\} = 0,$$

$$G^{\frac{1}{2}}u_t + M(1+u)u_x + \frac{1}{\gamma M(1+\rho)}p_x + \frac{M'}{G}\{(1+u)^2 - \frac{1+p}{1+\rho}\} = 0, \qquad (3.4)$$

$$G^{\frac{1}{2}}p_t + M(1+u)p_x - \frac{\gamma(1+p)}{1+\rho}\{G^{\frac{1}{2}}\rho_t + M(1+u)\rho_x\} = 0,$$

in which $M(x)$ is the Mach number of the basic steady flow, $U(x)/c_0(x)$, and

$$G(x) = c_s^2/c_0^2(x) = 1 + (\gamma-1)M^2/2. \qquad (3.5)$$

It will also be required to make use of the shock relations appropriate to discontinuous solutions $\bar{\rho}$, $\bar{u}$, and $\bar{p}$. These are (ref. 10),

$$-V[\bar{\rho}] + [\bar{\rho}\bar{u}] = 0,$$

$$-V[\bar{\rho}\bar{u}] + [\bar{\rho}\bar{u}^2 + \bar{p}] = 0, \qquad (3.6)$$

$$-V[\frac{\bar{\rho}\bar{u}^2}{2} + \frac{1}{\gamma-1}\bar{p}] + [\frac{\bar{\rho}\bar{u}^3}{2} + \frac{\gamma}{\gamma-1}\bar{p}\bar{u}] = 0,$$

in which V is the velocity of the shock, and the square brackets denote the jump in the enclosed quantity across the shock. Substituting the definitions (3.3) into conditions (3.6) and assuming that the basic steady flow is continuous leads to the jump conditions on the perturbation quantities in the form

$$-V[\rho] + U[\rho + u + \rho u] = 0,$$

$$-V[\rho + u + \rho u] + U[\rho + 2u + \frac{p}{\gamma M^2} + 2\rho u + u^2] + \ldots = 0,$$

$$-V[\frac{\rho}{2} + u + \frac{p}{\gamma(\gamma-1)M^2} + \rho u + \frac{u^2}{2}] \qquad (3.7)$$

$$+ U[(\frac{3}{2} + \frac{1}{(\gamma-1)M^2})u + \frac{\rho}{2} + \frac{p}{(\gamma-1)M^2} + \frac{3}{2}u^2$$

$$+ \frac{3}{2}\rho u + \frac{pu}{(\gamma-1)M^2}] + \ldots = 0,$$

where the terms omitted in the momentum and energy jump conditions are third-order products of the perturbation quantities which are not needed in the following.

It is assumed that the basic flow quantities R, U, and c_0 are known from solving the system (3.2) subject to suitable

boundary conditions applied far upstream and downstream of the
duct throat at x=0. Of interest in the present work is the solu-
tion of the quasi-linear system (3.4), which describes the per-
turbation quantities exactly, regardless of their magnitude. In
general these quantities will contain discontinuities whose mag-
nitude and space-time path are determined from the shock condi-
tions (3.7).

Because sound propagation in near-sonic flows is of interest
here, it will be assumed that the boundary conditions on the basic
steady flow are such that the throat Mach number is near unity.
A parameter $\varepsilon = 1 - M(0)$ is thus introduced into the analysis, and the
Mach number is henceforth regarded as a function of the parameter
ε as well as of x. In the analysis that follows ε will be assumed
to be positive: the basic flow is subsonic throughout the duct.
The coefficients in the system (3.4) and in the conditions (3.7)
then all become functions of ε, which implies that the perturba-
tion quantities are functions of ε. In the work which follows,
asymptotic solutions for ρ, u, and p will be derived in the limit
as $\varepsilon \to 0$. It has been shown in detail in previous publications by
the authors (refs. 2 - 5) that for $\varepsilon \ll 1$ the acoustic perturbation
field can be divided into two regions: an outer region away from
the throat where linear acoustic theory is a valid first approxi-
mation to the system (3.4), and an inner region around the throat
where nonlinear effects predominate. The essential results of the
previous analyses of the behavior of the acoustic quantities in
the outer region will be summarized in the following section.

Outer Expansions: Linearized Acoustic Theory

If it is assumed that the perturbation quantities ρ, u and p
are small, the system (3.4) can be linearized. Let δ be a small
parameter measuring the order of magnitude of the perturbations.
Expressing the perturbation quantities in powers of δ as

$$\rho(x,t;\varepsilon,\delta) = \delta \rho_1(x,t;\varepsilon) + 0(\delta^2),$$

$$u(x,t;\varepsilon,\delta) = \delta u_1(x,t;\varepsilon) + 0(\delta^2), \qquad (3.8)$$

$$p(x,t;\varepsilon,\delta) = \delta p_1(x,t;\varepsilon) + 0(\delta^2),$$

substituting equations (3.8) into equations (3.4), and neglecting
all but the terms proportional to δ yields the linearized acous-
tic equations

10

$$G^{\frac{1}{2}}\rho_{1_t} + M(\rho_{1_x} + u_{1_x}) = 0,$$

$$G^{\frac{1}{2}}u_{1_t} + Mu_{1_x} + \frac{1}{\gamma M} p_{1_x} + \frac{M'}{G}(2u_1 + \rho_1 - p_1) = 0, \qquad (3.9)$$

$$G^{\frac{1}{2}}p_{1_t} + Mp_{1_x} - \gamma(G^{\frac{1}{2}}\rho_{1_t} + M\rho_{1_x}) = 0.$$

In general, the system (3.9) would have to be solved numerically, subject to appropriate boundary and initial conditions, because of its variable coefficients. For the present purposes, however, since $\varepsilon \ll 1$, a further expansion of the perturbation quantities is carried out such that

$$\rho_1(x,t;\varepsilon) = \rho_0(x,t) + 0(\varepsilon),$$

$$u_1(x,t;\varepsilon) = u_0(x,t) + 0(\varepsilon),$$

$$p_1(x,t;\varepsilon) = p_0(x,t) + 0(\varepsilon),$$

where the quantities ρ_0, u_0, and p_0 satisfy the linear system (3.9) with the coefficient terms $M(x;\varepsilon)$ and $G(x;\varepsilon)$ replaced by

$$M_0(x) = M(x;0) \text{ and } G_0(x) = G(x;0).$$

As has been discussed previously (ref. 1), the function $M_0(x)$ is any Mach number distribution such that $M_0(0)=1$ and $M_0(x)<1$ throughout the remainder of the duct. In general, $M_0(x)$ has the expansion for $x \ll 1$ (ref. 1)

$$M_0(x) = 1 - \{\frac{\gamma+1}{2} a\}^{\frac{1}{2}}|x| + 0(x^2) \qquad (3.10)$$

in which $a = A''(0)/2A(0) > 0$.

The solution for ρ_0, u_0 and p_0 for a general area distribution has been discussed extensively by the authors (refs. 1,5). For the present work, however, a specific duct shape will be chosen for which the authors obtained an analytical solution by extending a result of Crocco and Tsien (ref. 1). The Mach number distribution for the Crocco-Tsien duct is given for all x by

$$M_0(x) = (1-K|x|)\{\frac{\gamma+1}{2} - \frac{\gamma-1}{2}(1-K|x|)^2\}^{-\frac{1}{2}}, \ |x| < \frac{1}{K}.$$

Near $x=0$ this assumes the form of equation (3.10) with $K^2 = 2a/(\gamma+1)$. If a dimensionless frequency ω, measured in units of c_s/L is introduced, then complex periodic solutions to the system (3.9) to leading order in ε are

$$\rho_0 = \sum_{n=0}^{\infty} \{A_{1n} G_{1n}(x) + B_{1n} G_{2n}(x)\} e^{in\omega t}$$

$$(3.11)$$

$$u_0 = \sum_{n=0}^{\infty} \{A_{1n} G_{3n}(x) + B_{1n} G_{4n}(x)\} e^{in\omega t}$$

$$p_0 = \gamma \rho_0,$$

where A_{1n} and B_{1n} are arbitrary complex constants, and the G_{in}, $i=1,\ldots, 4$, are combinations of hypergeometric functions of complex argument whose explicit forms are given in the appendix. The local behavior of the G_{in} as $x \to 0$ has been shown to be (refs. 1,5),

$$G_{1n} \sim \left(\frac{1}{|x|} + c_{11}\right) \exp\left(\frac{in\omega}{a^{\frac{1}{2}}} \, \mathrm{sgn}\, x \, \ln|x|\right)$$

$$G_{2n} \sim 1$$

$$G_{3n} \sim \left(-\frac{1}{|x|} + c_{12}\right) \exp\left(\frac{in\omega}{a^{\frac{1}{2}}} \, \mathrm{sgn}\, x \, \ln|x|\right)$$

$$(3.12)$$

$$G_{4n} \sim d_{02}$$

where the constants c_{11}, c_{12}, and d_{02} appear also in the appendix.

The local expansion (3.12) provides the key to the analysis of the acoustic behavior of the converging-diverging duct. The acoustic quantities are given by

$$\rho = \delta \rho_0(x,t) + O(\varepsilon\delta)$$

$$u = \delta u_0(x,t) + O(\varepsilon\delta)$$

$$(3.13)$$

$$p = \delta \gamma \rho_0(x,t) + O(\varepsilon\delta)$$

in the limit as $\varepsilon \to 0$. For any δ, no matter how small, the linearized theory fails to approximate the perturbation quantities near the throat as the Mach number there approaches unity. Equations (3.12) show that the leading terms ρ_0, u_0, and p_0 of the expansions (3.13) become arbitrarily large in this circumstance, thereby violating the assumption made in deriving the system (3.9) that they remain small. Numerical solutions of the system (3.9) which illustrate the growth of these large amplitudes were presented in reference 1.

12

Thus the interpretation of the role of linearized acoustic theory in the current problem is clear. The expansion (3.8) is to be regarded as an outer asymptotic expansion, valid as $\delta \to 0$ with x, t, and ε fixed. The result (3.12) shows that it is not uniformly valid as $x \to 0$ and $\varepsilon \to 0$. Hence, in the vicinity of the duct throat, nonlinear effects become important as the flow approaches sonic conditions. The correct nonlinear theory which must be used to describe sound in the near-sonic throat flow will be presented in the next chapter.

4. NONLINEAR THEORY

Inner Expansions

The preceding results indicate that linearized theory fails to describe properly the propagation of sound in the vicinity of a near-sonic throat. As has been discussed previously (refs. 2-5), the size of the region around $x=0$ in which the outer expansions fail is of $0(\varepsilon)$. Therefore a "stretched" or inner variable

$$X = [\frac{(\gamma+1)a}{2}]^{\frac{1}{2}} \frac{x}{\varepsilon} \tag{4.1}$$

and a modified time variable $T = a^{\frac{1}{2}}t$ are introduced, and the solution to the systems (3.2), (3.4), and (3.6) is examined in the inner region, $X=0(1)$. The factor $a^{\frac{1}{2}}$ in X and T is included for convenience in order that a does not appear explicitly in the subsequent analysis. The basic flow Mach number in the inner region has the expansion (refs. 1,5)

$$M(x;\varepsilon) = M^i(X;\varepsilon) = 1 - \varepsilon m_1(X) + 0(\varepsilon^2) \tag{4.2}$$

in which $m_1(X) = (1 + X^2)^{\frac{1}{2}}$. The perturbation quantities are expanded in the form

$$\rho(x,t;\varepsilon) = \rho^i(X,T;\varepsilon) = \varepsilon r_1(X,T) + \varepsilon^2 r_2(X,T) + ...,$$

$$u(x,t;\varepsilon) = u^i(X,T;\varepsilon) = \varepsilon \mu_1(X,T) + \varepsilon^2 \mu_2(X,T) + ..., \tag{4.3}$$

$$p(x,t;\varepsilon) = p^i(X,T;\varepsilon) = \varepsilon \sigma_1(X,T) + \varepsilon^2 \sigma_2(X,T) + ...$$

Substitution of the expansions (4.2) and (4.3) into the system (3.4), changing the spatial variable to X, and equating the coefficients of each power of ε to zero following the same steps as in reference 2 yields at the lowest order

$$r_{1_X} + \mu_{1_X} = 0, \tag{4.4}$$

$$(\mu_1 - \frac{1}{\gamma} \sigma_1)_T + (2\mu_1 + r_1 - \sigma_1 - 2m_1)\mu_{1_X}$$

$$-\frac{2m_1'}{\gamma+1} (2\mu_1 + r_1 - \sigma_1) = 0, \tag{4.5}$$

$$\sigma_{1_X} - \gamma r_{1_X} = 0. \tag{4.6}$$

14

For later purposes it will be necessary to use the second order counterpart of the inner equation of continuity (4.4), which is

$$r_{2_X} + \mu_{2_X} = -r_{1_T} - \mu_1 r_{1_X} - r_{1_X} - r_1 \mu_{1_X}. \qquad (4.7)$$

The corresponding inner form of the shock conditions (3.6) can be obtained using the expansions (4.2) and (4.3) and by representing the unknown shock location in the form

$$T = H(x;\varepsilon) = H_0(X) + \varepsilon H_1(X) + \dots .$$

Since t and x are scaled according to L/c_S and L, respectively, this yields the expression for the shock velocity V, which is to be determined in the course of the analysis, as

$$V = (\frac{2}{\gamma+1})^{\frac{1}{2}} \frac{\varepsilon c_S}{H_0'(X)} + 0(\varepsilon^2). \qquad (4.8)$$

Equations (4.2), (4.3), and (4.8) are substituted into the equations (3.6) and the coefficients of each power of ε equated to zero to yield the lowest order shock conditions on the inner solution in the form

$$[r_1 + \mu_1] = 0, \qquad (4.9)$$

$$[r_1 + 2\mu_1 + \frac{1}{\gamma} \sigma_1] = 0, \qquad (4.10)$$

$$[\mu_1 - \frac{1}{\gamma} \sigma_1] + H_0'[\frac{\gamma-3}{2} \mu_1^2 - r_1\mu_1 + \sigma_1\mu_1 + 2m_1\mu_1] = 0. \qquad (4.11)$$

The quasi-linear system (4.4-4.6) describes the behavior of sound propagating in the near-sonic duct throat region to leading order in the small parameter ε. It expresses the fact that the sound propagation process is inherently nonlinear in the near-sonic flow. Solutions to this system will be discussed in the following, where it will be seen that in general discontinuities in the quantities r_1, μ_1, and σ_1 will develop. The magnitude of these discontinuities as well as their unknown location $T=H_0(X)$ will be determined using the shock conditions (4.9-4.11).

Boundary Conditions

The theory outlined in the preceding sections will be applied in the following to study the sound field propagating upstream in a Crocco-Tsien duct. For convenience, the upstream exit of the duct at $x = x_e < 0$ will be assumed anechoic. It is known (ref. 3)

15

that vanishing of the downstream propagating wave at a point in the outer region requires $M_0 u_{0n} + p_{0n} = 0$ there. Thus, the anechoic end condition will relate the complex constants A_{1n} and B_{1n} in the outer solution (3.11) in $x < 0$ according to

$$\frac{\bar{B}_{1n}}{\bar{A}_{1n}} = - \frac{M_0(x_e)G_{3n}(x_e) + G_{1n}(x_e)}{M_0(x_e)G_{4n}(x_e) + G_{2n}(x_e)} . \qquad (4.12)$$

The superscript on the constants in equation (4.12) is used to indicate that these are the constants appropriate to the linear solution (3.11) in $x < 0$. On the downstream side of the throat the constants will, in general, be different and will be denoted A_{1n}^+, B_{1n}^+ when necessary.

The remaining boundary condition is an acoustic source condition. Here it will be assumed that the source is located at $x = x_0$, and that the perturbation velocity there is specified, i.e.,

$$U(x; \varepsilon)u(x_0, t; \varepsilon) = c_0(x_0)M_0(x_0; \varepsilon)u(x_0, t; \varepsilon) = S \sin \omega t$$

where $S/c_0(x_0) << 1$. Two cases arise according as the point $x = x_0$ lies in the inner region, $x_0 = 0(\varepsilon)$, or in the outer region, $x_0 = 0(1)$. In the former case, the source amplitude is required to be proportional to ε, so that the boundary condition becomes

$$c_0(\varepsilon X_0)M^i(X_0; \varepsilon)u^i(X_0, T; \varepsilon) = \varepsilon \hat{U} \sin \Omega T,$$

where the modified frequency $\Omega = \omega/a^{\frac{1}{2}}$ has been introduced and where $\hat{U}$ is a constant. The inner point $X_0 = \{\frac{(\gamma+1)a}{2}\}^{\frac{1}{2}} \frac{x_0}{\varepsilon} = 0(1)$. Using Equations (3.5), (4.2), and (4.3), the source condition on the leading order inner problem becomes

$$\mu_1(X_0, T) = \frac{2}{\gamma+1} N \sin \Omega T \qquad (4.13)$$

where

$$N = (\frac{\gamma+1}{2})^{3/2} \frac{\hat{U}}{c_s}.$$

On the other hand, if the acoustic source is located downstream of the throat in the outer region the amplitude S will be taken to be of $0(\delta)$, consistent with the definition of δ as the perturbation level in this region. In this case the source condition becomes

$$c_0(x_0)M(x_0;\varepsilon)u(x_0,t;\varepsilon) = \delta c_0(x_0)M_0(x_0)u_0(x_0,t)+\ldots = \delta\tilde{U}\sin\omega t.$$

In this situation the boundary condition on the leading order solution in the outer region is

$$u_0(x_0,t) = \tilde{N}\sin\omega t \qquad (4.14)$$

in which $\tilde{N} = \tilde{U}/c_0(x_0)M_0(x_0)$. Using the solution (3.11) in $x>0$, the condition (4.14) yields relationships between the complex constants A_{1n}^+ and B_{1n}^+ in the form,

$$B_{1n}^+ - R_n^+(x_0)A_{1n}^+ = F_n,$$

where the complex constants $F_n=0$ if $n\neq1$, and F_1 is proportional to N. It is easily verified using Equation (3.11) that

$$R_n^+(x_0) = G_{3n}(x_0)/G_{4n}(x_0).$$

In the specific results derived later the major emphasis is on the problem for which the acoustic source lies in the inner region, $x_0=0(\varepsilon)$, so that the source condition is as in Equation (4.13). The reason for this emphasis is that the throat source problem can be solved analytically. Thus it offers an overwhelming advantage for gaining insight into the nonlinear effects of the near-sonic flow on sound. In reference 4 the authors discussed the more practically interesting latter case, for which condition (4.14) is relevant, under the restriction that shocks do not form. The complete solution in this case involves a complicated iteration scheme. The generalization of this scheme to include the development of shocks will be the subject of a future publication.

5. SOLUTION OF THE INNER PROBLEM: ACOUSTIC SOURCE NEAR THE THROAT

The solution of the system (4.4-4.6) subject to the shock conditions (4.9-4.11), the boundary condition (4.13), and appropriate asymptotic matching conditions to be discussed later can be effected most easily by introducing certain physical considerations to reduce the complexity of the problem.

Reduction to a Signaling Problem

It has been shown in references 3 and 5 that the combination $r_1 + \mu_1$ is the leading order inner representation of the downstream propagating Riemann variable for the system (3.4). It satisfies the linear relation $(r_1 + \mu_1)_X = 0$ and is continuous in the inner region by virtue of condition (4.9). This, together with the fact that the combination $\rho_0 + u_0$ of the outer solution remains finite as $x \to 0$ (see eqs. (3.11) and (3.12)), suggests that the downstream propagating wave is unaffected at the lowest order by the nonlinearity in the inner region and that, in fact, $r_1 + \mu_1$ vanishes.

Also, since discontinuities in the inner solution represent shocks whose strength is $0(\varepsilon)$, it is anticipated that entropy changes occurring near the throat are of $0(\varepsilon^3)$. If so, the first order inner perturbation field is homentropic, and the appropriate solution of equation (4.6) is $\sigma_1 = \gamma r_1$.

Thus, it will be assumed here, and later verified by asymptotic matching, that $\mu_1 = -r_1$ and $\sigma_1 = \gamma r_1$. In this event, equations (4.4), (4.6), (4.9), and (4.10) are satisfied identically. The remaining inner equation of motion (4.5) and shock condition (4.11) reduce to

$$2\mu_{1_T} + \{(\gamma+1)\mu_1 - 2m_1\}\mu_{1_X} - 2m_1'\mu_1 = 0, \qquad (5.1)$$

and

$$[2\mu_1] + H_0' [-\frac{(\gamma+1)}{2} \mu_1^2 + 2m_1\mu_1] = 0. \qquad (5.2)$$

Finally if the definition

$$\Pi(X,T) = \frac{\gamma+1}{2} \mu_1(X,T) - m_1(X)$$

is introduced, the inner problem (5.1), (5.2), and (4.13) is transformed into the following signaling problem:

$$\Pi_T + \Pi\Pi_X = X, \quad -\infty < X < X_0, \qquad (5.3)$$

$$\Pi(X_0,T) = -(1 + X_0^2)^{\frac{1}{2}} + N \sin \Omega T, \qquad (5.4)$$

where discontinuities in Π occur on the space-time curves $T=H_0(X)$ and satisfy

$$2[\Pi] - H_0'[\Pi^2] = 0 \qquad (5.5)$$

Interest here is directed toward time-periodic or steady-state solutions. Hence, no initial conditions are stated, i.e., it is assumed that the source has been acting for a long period of time.

Equation (5.3) can be solved using the method of characteristics (ref. 11); it states that

$$\frac{d\Pi}{dT} = X \qquad (5.6)$$

along the characteristic curves in (X,T) which satisfy

$$\frac{dX}{dT} = \Pi \qquad (5.7)$$

A parameter τ is introduced such that τ = constant along a characteristic curve, and τ is chosen such that $\tau=T$ when $X=X_0$. Differentiation of equation (5.6) with respect to T holding τ fixed and use of equation (5.7) leads to

$$\frac{d^2\Pi}{dT^2} - \Pi = 0$$

along a characteristic. Hence Π is of the form

$$X = A(\tau) \sinh T + B(\tau) \cosh T.$$

Application of the boundary condition (5.4) and the condition $T=\tau$ on $X=X_0$ then yields the inner solution in the form

$$\Pi = \phi(\tau) \cosh (T-\tau) + X_0 \sinh (T-\tau), \qquad (5.8)$$

$$X = \phi(\tau) \sinh (T-\tau) + X_0 \cosh (T-\tau), \qquad (5.9)$$

in which

$$\phi(\tau) = N \sin \Omega\tau - (1+X_0^2)^{\frac{1}{2}}. \qquad (5.10)$$

Equations (5.8-5.9) are a parametric representation of the exact solution to the inner problem (5.3), (5.4). As will be seen in the following, this representation can be matched asymptotically to the outer solution even though it is not possible to express Π explicitly as a function of X and T.

The behavior of the inner solution (5.8) and (5.9) when $X_0=0$ has been discussed extensively in references 3 and 5 under the restriction that Π remains continuous over $-\infty < X < 0$. Here,

however, solutions which develop shocks are of primary interest. Shocks occur in the solution Π whenever the one-parameter family of characteristic curves (5.9) overlap in the (X,T) plane, thereby rendering the expression (5.8) for Π multivalued. The condition for the occurrence of such multivaluedness follows from the fact that the boundary of a region of overlap must be an envelope of the family of characteristic curves. An envelope, if one exists, is given by simultaneous solution of equation (5.9) with its derivative with respect to τ:

$$\phi(\tau) \cosh (T-\tau) - (\phi'(\tau) - X_0) \sinh (T-\tau) = 0. \qquad (5.11)$$

Now, in the present problem, only those characteristics propagating upstream from $X=X_0$ can carry the solution through the throat region; i.e. $dX/dT < 0$ at $X=X_0$ on all characteristics of interest. Equation (5.7) then indicates that $\Pi<0$ on each of these. Since $\Pi=\phi$ at $X=X_0$ it follows that $\phi<0$ on every characteristic propagating upstream from the source. Now, $T-\tau>0$ on any such characteristic, and hence equation (5.11) implies that $\phi'-X_0<0$ and that $\phi/(\phi'-X_0)<1$ on all characteristic curves which overlap and form an envelope. The second of these conditions provides the criterion for the development of shocks in the inner solution Π: shocks will form if and only if

$$\phi'(\tau) - X_0 < \phi(\tau) \qquad (5.12)$$

for some range of τ between, say, $\tau=0$ and $\tau=2\pi/\Omega$. The inequality (5.12) is the condition on source strength, frequency, and location such that the inner solution Π will develop shocks.

Using equation (5.10), the condition (5.12) implies

$$N(\sin \Omega\tau - \Omega \cos \Omega\tau) > (1+X_0^2)^{\frac{1}{2}} - X_0.$$

If the left side of this inequality is maximized with respect to τ it follows that it can be satisfied for some range of τ over each period if and only if

$$N(1+\Omega^2)^{\frac{1}{2}} > (1+X_0^2)^{\frac{1}{2}} - X_0 \qquad (5.13)$$

Equation (5.13) is the specific relation for the present problem which determines in terms of the given parameters whether the nonlinear inner perturbation field develops discontinuities. It was derived for the special case $X_0=0$ in references 2,5 and 6.

Wherever N, Ω, and X_0 satisfy condition (5.13), the upstream propagating wave represented by Π will steepen and break in typical nonlinear fashion. Breaking first occurs at the point (X,T) where the envelope of characteristics forms a cusp. The characteristic τ through the cusp is determined by eliminating T between equation (5.11) and its derivative with respect to τ:

$$(2\phi'(\tau)-X_0) \cosh (T-\tau) - (\phi''(\tau) + \phi(\tau)) \sinh (T-\tau) = 0.$$

Consideration of the simultaneous solution of this equation along

with equations (5.9) and (5.11) shows that, for N slightly greater than the critical value indicated in equation (5.13), the cusp is located at large negative X. Also, using the same three equations it can be seen that the cusp will lie on $X=X_0$ only if $\phi(\tau)=0$ and $2\phi'(\tau)-X_0=0$, i.e., if

$$N \sin \Omega\tau = (1 + X_0^2)^{\frac{1}{2}} \text{ and } 2N\Omega \cos \Omega\tau = X_0,$$

which requires that

$$N = N_c = (1 + X_0^2 + X_0^2/4\Omega^2)^{\frac{1}{2}}. \tag{5.14}$$

With the information developed thus far it is possible to establish clearly a qualitative picture of the development of shocks in the perturbation field arising from nonlinear interactions near the duct throat. In general, the inequality (5.13) indicates that shocks will form as any of the parameters N, Ω, and X_0 increases. For the present discussion Ω and X_0 will be considered fixed. Then for sufficiently small N the solution is continuous, as in references 3 and 5. As N is increased beyond the value indicated in equation (5.13), a shock wave occurs in each period of the inner solution II. Provided N is less than the value N_c of equation (5.14) the shock starts with zero strength at a finite distance upstream of $X=X_0$, where the steepening wave profile first develops an infinite slope. As N increases towards N_c the shock formation point moves back towards $X=X_0$. For $N>N_c$ no cusp forms on the envelope of characteristics in $X<X_0$. In this case, as will be discussed in more detail later, the shock forms directly at the source, $X=X_0$.

The actual characteristics over $0 \leq \tau < 2\pi/\Omega$, given by equations (5.9) and (5.10) for the present problem, are shown plotted in figures 2(a) to 2(d) for the case $X_0=1$, $\Omega=1$. In this instance, the shock exists for $N>.222$, and the value of N_c is 1.5. These figures will be discussed in detail later, but for the present it is of interest to note that as N increases towards N_c the cusp turns so that the slope of the envelope (and thus of the shock) becomes positive there. That is, the shock actually travels downstream towards the source after its inception. Because of this, there is a range of N slightly below N_c in which the shock forms with zero strength at the cusp, travels downstream to interact with the source, and than proceeds back upstream through the throat.

Shock Fitting

The multivaluedness predicted by equations (5.8) and (5.9) is resolved by the introduction of appropriate discontinuities which satisfy the jump relation (5.5). The approach to be used in this process is parallel to that of Whitham (ref. 10). However, the

inhomogeneous nature of the differential equation (5.3) signifi-
cantly complicates the analysis, owing mainly to the fact that the
characteristics are not straight and the solution Π does not re-
main constant along them. Fortunately, however, it is possible to
carry out the shock analysis analytically despite the complications.

Each point of a shock path in space-time is a point at which
two characteristic curves, carrying different values of Π, inter-
sect. Let the characteristic intersecting the shock from ahead
(i.e. from larger negative X) be labeled τ_2 and that intersecting
the shock from behind be τ_1. Then $\tau_1 \geq \tau_2$ on the shock. Using
equation (5.9), a point X on the two characteristics, and on the
shock, satisfies

$$X = X_0 \cosh (T-\tau_1) + \phi_1 \sinh (T-\tau_1), \qquad (5.15)$$

$$X = X_0 \cosh (T-\tau_2) + \phi_2 \sinh (T-\tau_2),$$

in which $\phi_1 \equiv \phi(\tau_1)$, $\phi_2 \equiv \phi(\tau_2)$. The shock condition (5.5) gives

$$\frac{dT}{dX} = H_0'(X) = \frac{2}{\Pi_1 + \Pi_2} \qquad (5.16)$$

where $\Pi_1 = \Pi(T;\tau_1)$, $\Pi_2 = \Pi(T;\tau_2)$. The three equations (5.15-5.16)
determine simultaneously the parameters $\tau_1(X)$ and $\tau_2(X)$ and the
path $T=H_0(X)$ along the shock.

It is now required to derive a generalization of the equal
area relation of weak shock theory using equations (5.15-5.16).
First, equations (5.15) are differentiated with respect to X along
the shock and added, which leads to

$$2 = \frac{dT}{dX} \{X_0 \sinh (T-\tau_1) + \phi_1 \cosh (T-\tau_1)$$

$$X_0 \sinh (T-\tau_2) + \phi_2 \cosh (T-\tau_2)\}$$

$$+ \frac{d\tau_1}{dX} \{-X_0 \sinh (T-\tau_1) + \phi_1' \sinh (T-\tau_1)$$

$$-\phi_1 \cosh (T-\tau_1)\}$$

$$+ \frac{d\tau_2}{dX} \{-X_0 \sinh (T-\tau_2) + \phi_2' \sinh (T-\tau_2)$$

$$-\phi_2 \cosh (T-\tau_2)\}.$$

The term multiplying $\frac{dT}{dX}$ in the above relation is seen using equation (5.8) to be $\Pi_1 + \Pi_2$; use of the shock condition (5.16) then reduces the result to

$$\Pi_1 \frac{d\tau_1}{dX} + \Pi_2 \frac{d\tau_2}{dX} = \phi_1' \sinh (T-\tau_1) \frac{d\tau_1}{dX} + \phi_2' \sinh (T-\tau_2) \frac{d\tau_2}{dX}. \quad (5.17)$$

It is to be shown that equation (5.17) can be integrated to yield an equation for $\tau_1(X)$ and $\tau_2(X)$. To do this requires first that the unknown function $T(X)$ be eliminated. This can be accomplished by using equations (5.8) and (5.9) to get

$$\sinh (T-\tau) = \frac{X\phi - X_0 \Pi}{\phi^2 - X_0^2} \quad (5.18)$$

$$\cosh (T-\tau) = \frac{\Pi\phi - XX_0}{\phi^2 - X_0^2} . \quad (5.19)$$

Equation (5.18) is now substituted into equation (5.17), and the equation is multiplied by $\Pi_1 - \Pi_2$ (which is non-zero in general), to obtain

$$(\Pi_1^2 - \Pi_1\Pi_2) \frac{d\tau_1}{dX} + (\Pi_1\Pi_2 - \Pi_2^2) \frac{d\tau_2}{dX}$$

$$= X(\Pi_1 - \Pi_2)\{ \frac{\phi_1 \phi_1'}{\phi_1^2 - X_0^2} \frac{d\tau_1}{dX} + \frac{\phi_2 \phi_2'}{\phi_2^2 - X_0^2} \frac{d\tau_2}{dX} \}$$

$$-X_0(\Pi_1^2 - \Pi_1\Pi_2) \{ \frac{\phi_1'}{\phi_1^2 - X_0^2} \frac{d\tau_1}{dX} + \frac{\phi_2'}{\phi_2^2 - X_0^2} \frac{d\tau_2}{dX} \} . \quad (5.20)$$

Using equations (5.8) and (5.9), it can be seen that

$$\Pi^2 - X^2 = \phi^2 - X_0^2 . \quad (5.21)$$

Thus the left side of equation (5.20) can be written as

$$\{\phi_1^2 - X_0^2 - (\Pi_1\Pi_2 - X^2)\} \frac{d\tau_1}{dX} + \{(\Pi_1\Pi_2 - X^2) - \phi_2^2 + X_0^2\} \frac{d\tau_2}{dX} ,$$

while the second term on the right side is

$$-X_0 \phi_1' \frac{d\tau_1}{dX} + \frac{X_0(\Pi_1\Pi_2-X^2)}{\phi_1^2-X_0^2} \phi_1' \frac{d\tau_1}{dX}$$

$$+ X_0\phi_2' \frac{d\tau_2}{dX} - \frac{X_0(\Pi_1\Pi_2-X^2)}{\phi_2^2-X_0^2} \phi_2' \frac{d\tau_2}{dX} \ .$$

Use of these two results allows equation (5.20) to be rearranged in the form

$$\phi_1^2 \frac{d\tau_1}{dX} - \phi_2^2 \frac{d\tau_1}{dX} = X_0^2(\frac{d\tau_1}{dX} - \frac{d\tau_2}{dX}) - X_0(\frac{d\phi_1}{dX} - \frac{d\phi_2}{dX})$$

$$+ X(\Pi_1^-\Pi_2)\{\frac{\phi_1\phi_1'}{\phi_1^2-X_0^2} \frac{d\tau_1}{dX} + \frac{\phi_2\phi_2'}{\phi_2^2-X_0^2} \frac{d\tau_2}{dX}\} \qquad (5.22)$$

$$+ (\Pi_1\Pi_2-X^2)\{\frac{d\tau_1}{dX} - \frac{d\tau_2}{dX} + \frac{X_0\phi_1'}{\phi_1^2-X_0^2} \frac{d\tau_1}{dX} - \frac{X_0\phi_2'}{\phi_2^2-X_0^2} \frac{d\tau_2}{dX}\} .$$

Now, it is easily shown, using equations (5.18) and (5.19) that

$$\cosh (\tau_1-\tau_2) = \cosh \{T-\tau_2 - (T-\tau_1)\}$$

$$= \frac{(\Pi_1\Pi_2-X^2)(\phi_1\phi_2-X_0^2)-XX_0(\phi_1-\phi_2)(\Pi_1-\Pi_2)}{(\phi_1^2-X_0^2)(\phi_2^2-X_0^2)} \ ,$$

and, similarly,

$$\sinh (\tau_1-\tau_2) = \frac{X(\Pi_1-\Pi_2)(\phi_1\phi_2-X_0^2) - X_0(\phi_1-\phi_2)(\Pi_1\Pi_2-X^2)}{(\phi_1^2-X_0^2)(\phi_2^2-X_0^2)} \ .$$

These two relations are considered as simultaneous algebraic equations for the quantities $X(\Pi_1-\Pi_2)$ and $(\Pi_1\Pi_2-X^2)$ whose solution is

$$X(\Pi_1-\Pi_2) = (\phi_1\phi_2-X_0^2) \sinh (\tau_1-\tau_2) + X_0(\phi_1-\phi_2) \cosh (\tau_1-\tau_2)$$

$$(5.23)$$

$$\Pi_1\Pi_2-X^2 = (\phi_1\phi_2-X_0^2) \cosh (\tau_1-\tau_2) + X_0(\phi_1-\phi_2) \sinh (\tau_1-\tau_2) .$$

Finally, equations (5.23) are substituted into equation (5.22). When this is done it is a matter of straightforward algebra to show that the coefficient of $\sinh(\tau_1-\tau_2)$ simplifies to

$$\phi_1'\phi_2 \frac{d\tau_1}{dX} + \phi_1\phi_2' \frac{d\tau_2}{dX} + X_0(\phi_1-\phi_2)(\frac{d\tau_1}{dX} - \frac{d\tau_2}{dX}),$$

while the coefficient of $\cosh(\tau_1-\tau_2)$ is

$$X_0\phi_1' \frac{d\tau_1}{dX} - X_0\phi_2' \frac{d\tau_2}{dX} + (\phi_1\phi_2 - X_0^2)(\frac{d\tau_1}{dX} - \frac{d\tau_2}{dX}).$$

Equation (5.22) then becomes

$$\phi_1^2 \frac{d\tau_1}{dX} - \phi_2^2 \frac{d\tau_2}{dX} = X_0^2 \frac{d}{dX}(\tau_1-\tau_2) - X_0 \frac{d}{dX}(\phi_1-\phi_2)$$

$$+ \{\frac{d}{dX}(\phi_1\phi_2) + X_0(\phi_1-\phi_2)\frac{d}{dX}(\tau_1-\tau_2)\}\sinh(\tau_1-\tau_2)$$

$$+ \{X_0\frac{d}{dX}(\phi_1-\phi_2) + (\phi_1\phi_2 - X_0^2)\frac{d}{dX}(\tau_1-\tau_2)\}\cosh(\tau_1-\tau_2),$$

which can now be seen directly to be

$$\frac{d}{dX}\int_{\tau_2}^{\tau_1}\phi^2 d\tau = X_0^2\frac{d}{dX}(\tau_1-\tau_2) - X_0\frac{d}{dX}(\phi_1-\phi_2)$$

$$+ \frac{d}{dX}\{(\phi_1\phi_2 - X_0^2)\sinh(\tau_1-\tau_2) + X_0(\phi_1-\phi_2)\cosh(\tau_1-\tau_2)\}.$$

Hence, equation (5.17) is equivalent to

$$\int_{\tau_2}^{\tau_1}\phi^2 d\tau = X_0^2(\tau_1-\tau_2) - X_0(\phi_1-\phi_2) + (\phi_1\phi_2 - X_0^2)\sinh(\tau_1-\tau_2)$$

$$+ X_0(\phi_1-\phi_2)\cosh(\tau_1-\tau_2) + D, \tag{5.24}$$

where D is a constant of integration to be determined presently. Equation (5.24) is the generalization to the present problem of the so-called equal area relation of weak shock theory (ref. 9). It is a transcendental relation between $\tau_1(X)$ and $\tau_2(X)$ on the shock, which, together with equations (5.15), completely determines the location and strength of the shock in the inner region.

Analysis of Characteristics and Shock Formation

The determination of the constant D (eq.(5.24)), which depends on the parameters N, Ω, and X_0, requires a detailed analysis of he configuration of the characteristic curves. These are illustrated (over one period) in figure 2 a-d for increasing values of N with $X_0=\Omega=1$. The circular symbols denote points on the envelope, calculated using equations (5.9) and (5.11). It can be seen from equation (5.9), and also from the figure, that so long as $-\phi(\tau)<X_0$, there exists a set of characteristics whose slope decreases towards negative infinity at some $X<X_0$ at a time which is easily found from equation (5.9) to be $T=\tau+\tanh^{-1}(-\phi(\tau)/X_0)$. Each of these characteristics is a hyperbolic cosine curve, symmetric about its turning point, which therefore returns to intersect the source line $X=X_0$ at

$$ T = \tau + 2 \tanh^{-1}(-\phi(\tau)/X_0) . \qquad (5.25) $$

Equation (5.25) can also be found directly from equation (5.9) by setting $X=X_0$ and using the identities relating sinh z and cosh z to tanh $\frac{1}{2}z$. The value of Π, which vanishes at the turning points, becomes positive on the downstream propagating portion of the cosh curves.

It can be shown that the combined Mach number $U(1+u)/c_0$ is equal to $1+\epsilon\Pi$ in the inner approximation. Hence, when a characteristic assumes a positive slope it means that the net flow (steady flow plus acoustic perturbation) is supersonic. The turning of the characteristics seen in figure 2 therefore represents an actual acoustic choking of the duct flow whereby sound imparted to the flow during portions of the period when the source amplitude is sufficiently low is prevented from propagating upstream through the throat. This choking phenomenon significantly complicates the analysis of the development of shock waves in the duct.

For N sufficiently small, the shock must first form at the point in $X<X_0$ at which the envelope of characteristics forms a cusp (see figures 2(a) and (b)). At such a point, $\tau_1=\tau_2$ must be a root of equation (5.24), which implies that D=0. As seen in figure 2(b),however, when N increases towards N_c the shock assumes a positive slope at its inception and initially travels downstream towards the source. Provided that it turns back upstream before

26

reaching $X=X_0$ the value of D remains zero. The condition that
the shock turn exactly at $X=X_0$ requires that $\tau_1=T$, and that
$\Pi(\tau_1)+\Pi(\tau_2)=0$. It follows from equations (5.25) and (5.8) that
$\Pi(\tau_2)=-\phi(\tau_2)$ at $X=X_0$, so that $\phi(\tau_1)=\phi(\tau_2)$. Thus

$$\tau_1^* = \pi/\Omega - \tau_2^*$$

$$\tau_1^* = \tau_2^* + 2\tanh^{-1}(-\phi(\tau_2^*)/X_0)$$

are the two equations which determine the characteristics τ_1^*, τ_2^*
intersecting on the shock when it reaches $X=X_0$ with zero velocity.
But these values also satisfy equation (5.24) with D=0, which
yields the upper limiting value of N=N* for which D=0. It does
not appear possible to derive a simple analytical result express-
ing N* in terms of X_0 and Ω. However, numerical solution of the
two above equations together with equation (5.24) in the case
$X_0=\Omega=1$ yields the result N*=1.12717 (the value of N_c in this case
is 1.50). The general configuration of the shock near $X=X_0$ is
indicated schematically in figure 3(a) and (b), where the envelope
of characteristics is shown by dashed lines, and the shock is in-
dicated by a heavy line. The picture, of course, is repeated pe-
riodically in T.

In the following discussion the form assumed by equation
(5.24) when the shock intersects the source line $X=X_0$ will be
needed. At any time at which the shock is at X_0 the value of τ_1
equals T and the value of τ_2 is that appropriate to the returning
branch of the cosh characteristic at that T; i.e., τ_2 (see eq.
(5.25)) is given by

$$\tau_1 = \tau_2 + 2\tanh^{-1}(-\phi_2/X_0). \tag{5.26}$$

Use of equations (5.18) and (5.19) with $\Pi_2=-\phi_2$ and $X=X_0$ yields

$$\sinh(\tau_1-\tau_2) = \frac{2X_0\phi_2}{\phi_2^2-X_0^2}, \tag{5.27}$$

$$\cosh(\tau_1-\tau_2) = \frac{-(\phi_2^2+X_0^2)}{\phi_2^2-X_0^2}. \tag{5.28}$$

If equations (5.27) and (5.28) are substituted into equation (5.24)
it becomes

$$\int_{\tau_1}^{\tau_2} (\phi^2 - X_0^2) \, d\tau = 2X_0\phi_2 + D. \tag{5.29}$$

Equation (5.29) is the form of the generalized equal area relation (5.24) when the shock is at $X=X_0$.

For $N^* < N < (1+X_0^2)^{\frac{1}{2}}$ the upper branch of the envelope moves towards $X=X_0$ until it actually touches the source line when $N=(1+X_0^2)^{\frac{1}{2}}$. The details of the characteristic picture are not visible on the scale of the actual plots used in figure 2. They are shown schematically in highly exaggerated form for the case $N=(1+X_0^2)^{\frac{1}{2}}$ in figure 3(c). Over this range of N the shock starts at the cusp, travels downstream, and intersects the source line with a nonzero velocity. Thus, the shock splits into two branches. On the lower branch, which includes the cusp, the value of D in equation (5.24) is zero. The characteristics τ_+ and τ_- indicated on the figure are the two which intersect on the lower branch of the shock at $X=X_0$. They are determined by simultaneous solution of equation (5.28) with D=0 and equation (5.26) using $\tau_1 = \tau_+$ and $\tau_2 = \tau_-$. It is noted that this lower branch of the shock is actually very short. In the case illustrated in figure 2, $X_0=1$ and the cusp is located at about $X=0.999$.

Directly above $T=\tau_+$ the solution Π is determined on $X=X_0$ not by the source data but rather by the values appropriate to the returning cosh characteristics $\tau \leq \tau_-$. Over this region the transformation relating τ to T is given by equation (5.25). Here the acoustic choking of the flow has extended all the way back to the source line $X=X_0$. The source, whose amplitude is insufficient to overcome the oncoming supersonic flow which it experiences, is completely blocked from imparting sound in the upstream direction. This suggests the physical argument which determines the value of D appropriate to the upper branch of the shock, which is the branch which actually travels back upstream towards $X=-\infty$. The shock must begin at the point $T=\tau_1^0$ at which the source amplitude ϕ (which is negative) exactly cancels the value of Π on the returning characteristic τ_2^0 to yield sonic conditions in the flow and a shock velocity of zero. This occurs just as in the previous determination of N^* only if $\phi(\tau_1^0)=\phi(\tau_2^0)$ and if equation (5.26) is satisfied by τ_1^0 and τ_2^0. Thus,

$$\tau_1^0 = \pi/\Omega - \tau_2^0,$$

$$\tau_1^0 = \tau_2^0 + 2\tanh^{-1}(-\phi_2^0/X_0),$$

where $\phi_2^o \equiv \phi(\tau_2^o)$, are the two equations which determine the characteristic curves intersecting at the initial point of the upper branch of the shock. The physical argument above is supported by detailed numerical studies performed by the authors which show that there is one and only one such value $\tau_1^o > \pi/2\Omega$ at which the above two equations are satisfied.

Once τ_1^o and τ_2^o are known from the above equations then D is determined for the upper branch of the shock by using equation (5.29):

$$D = \int_{\tau_2^o}^{\tau_1^o} (\phi^2 - X_0^2) \, d\tau - 2X_0\phi_2^o. \qquad (5.30)$$

For the range $(1+X_0^2)^{\frac{1}{2}} < N < N_c$ the characteristics appear as in figure 2(c). A schematic representation of their behavior near $X=X_0$ is shown on figure 3(d). The only difference between this and figure 3(c) is that there exists a range $\tau_0^- < T < \tau_0^+$ over which $\phi > 0$, where

$$\tau_0^- = \sin^{-1} \left(\frac{1-X_0^2}{N}\right)^{\frac{1}{2}} \quad \text{and} \quad \tau_0^+ = \pi/\Omega - \tau_0^-.$$

The envelope of characteristics has split (see figure 2(c)), but there still exists a cusp as indicated in figure 3(d). The values τ_+, τ_-, τ_1^o and τ_2^o are determined exactly as above, and D is given for the upper branch of the shock by equation (5.30).

For $N > N_c$ the cusp no longer exists, as was described earlier; the lower branch of the envelope, and hence the shock, disappears. This is illustrated by the plot of figure 2(d). Although no corresponding schematic is shown in figure 3, the upper branch of the shock starts at $X=X_0$ exactly as illustrated in figure 3(d). The values of τ_1^o, τ_2^o and D are determined as above.

In the asymptotic matching to be discussed in the following chapter, the value of D on the shock which propagates to large negative X is required in order to use equation (5.24) to find the limiting values of τ_1 and τ_2 as $X \to -\infty$. This is what has been determined in the preceding rather lengthy analysis. For the remainder of this work the integration constant for equation (5.24) will be denoted D(N), where $D(N) \equiv 0$ for $N < N^*$, and D(N) is given by equation (5.30) for $N > N^*$.

For the special case $X_0 = 0$ it is easily shown that $N^* = 1$ and that equation (5.30) yields

29

$$\Omega D(N) = (1 + \frac{N^2}{2})(\pi - 2\sin^{-1}\frac{1}{N}) - 3(N^2-1)^{\frac{1}{2}}$$

for N>1. In this case no lower shock branch ever appears.
This result was derived previously in reference 6. The numerical
examples to be discussed later are restricted to this special case.
The shock relations are used in the form of equation (5.24) and
the first of equations (5.23). For a fixed X the two equations
are solved using a Newton-Raphson procedure. Once $\tau_1(X)$ and
$\tau_2(X)$ are known then $T = H_0(X)$ is calculated using one of equations
(5.15).

6. ASYMPTOTIC MATCHING

The solution to the inner problem has been completely determined in the preceding chapter. This solution must be asymptotically matched to the outer solution to determine the perturbation level ρ of the acoustic field which propagates upstream from the throat and the constants A_{1n} and B_{1n} of equation (3.11). The matching will be carried out on the perturbation velocity u; corresponding results for ρ and p follow.

The one-term outer expansion of u is $u_1(x,t;\varepsilon)$. A one-term inner expansion of this follows by introducing the inner variable X so that $u \sim \delta u_1(x(X;\varepsilon), t;\varepsilon)$, and expanding to leading order in ε keeping X fixed. This is equivalent to a leading order expansion of u_1 for small x and ε, which is precisely the limit u_0 given by equations (3.11) and (3.12). Thus

$$u \sim \frac{-\delta}{|x|} \sum_{n=0}^{\infty} A_{1n}^{-} \exp\{in\omega(t - \frac{1}{a^{\frac{1}{2}}} \ln|x|)\}.$$

Finally, the physical value of u is the real part of this expression. Writing $A_{1n}^{-} = A_n \exp(in\omega\psi_n)$, this yields for the one-term inner expansion of the one-term outer expansion of u the expression

$$u \sim \frac{-\delta}{|x|} \sum_{n=0}^{\infty} A_n \cos n\omega(t - \frac{1}{a^{\frac{1}{2}}} \ln|x| + \psi_n). \tag{6.1}$$

The one-term inner expansion of u is, from equation (4.3),

$$u \sim \varepsilon\mu_1 = \frac{2\varepsilon}{\gamma+1}\{(1 + X^2)^{\frac{1}{2}} + \Pi(X,T)\}.$$

A one term outer expansion of this is derived by using equations (4.1) and (5.21) and expanding each term to leading order in ε keeping x fixed. Thus

$$\Pi = -\{\phi^2 - X_0^2 + X^2\}^{\frac{1}{2}} \sim -\{\frac{\gamma+1}{2}a\}^{\frac{1}{2}} \frac{|x|}{\varepsilon}\{1 + \frac{\phi^2-X_0^2}{(\gamma+1)a}\frac{\varepsilon^2}{x^2} + \cdots\}$$

$$(1 + X^2)^{\frac{1}{2}} \sim \{\frac{\gamma+1}{2}a\}^{\frac{1}{2}} \frac{|x|}{2}\{1 + \frac{1}{(\gamma+1)a}\frac{\varepsilon^2}{x^2} + \cdots\},$$

which yields

$$u \sim \frac{\varepsilon^2}{|x|} \frac{a}{2}\{\frac{\gamma+1}{2}a\}^{-3/2}\{1 - (\phi^2 - X_0^2)\}. \tag{6.2}$$

In conjunction with this result, the outer representation of the characteristic curves can be determined by similarly expanding equation (5.18). This results in

$$T \equiv a^{\frac{1}{2}}t = \tau - \ell n \, |\phi(\tau) + X_0| + g(x;\varepsilon) \qquad (6.3)$$

to leading order, where

$$g(x;\varepsilon) = \ell n \, 2(\frac{\gamma+1}{2} a)^{\frac{1}{2}} \frac{|x|}{\varepsilon} \, .$$

It is noted that in deriving equation (6.3) use has been made of the fact that as $X \to -\infty$ both Π and ϕ are negative on the characteristic curve. Since $(T-t)>0$, equation (5.18) implies that $\phi^2 - X_0^2 > 0$. It follows that $\phi + X_0 < 0$ on each characteristic which extends to large negative X.

Equation (6.2) is the one-term outer expansion of the one-term inner expansion of u expressed in parametric form, where the parameter τ is defined in terms of x,t by equation (6.3).

Now, because $\phi(\tau)$ is a periodic function of τ (see equation (5.10)), and $T-\tau$ is a periodic function of τ, it follows that $\phi^2(\tau)$ is a periodic function of T with period $2\pi/\Omega$ and thus of t with period $2\pi/\omega$. Hence $\phi^2(\tau)$ can be written in the outer region as a Fourier series. It is convenient to include X_0^2 in the expansion and write

$$\phi^2(\tau) - X_0^2 = \frac{C_0(x)}{2} + \sum_{n=1}^{\infty} C_n(x) \cos n\omega t + D_n(x) \sin n\omega t$$

where

$$\begin{Bmatrix} C_n \\ D_n \end{Bmatrix} = \frac{\omega}{\pi} \int_0^{2\pi/\omega} (\phi^2(\tau) - X_0^2) \begin{Bmatrix} \cos n\omega t \\ \sin n\omega t \end{Bmatrix} dt$$

$$= \frac{\Omega}{\pi} \int_0^{2\pi/\Omega} (\phi^2(\tau) - X_0^2) \begin{Bmatrix} \cos n\Omega T \\ \sin n\Omega T \end{Bmatrix} dT \qquad (6.4)$$

To carry out an explicit evaluation of the Fourier coefficients it is necessary to consider the shock relations (5.23) and (5.24). In the outer limit, as $X \to -\infty$, it is easy to show from equation (5.21) that

$$X(\Pi_1 - \Pi_2) \sim \frac{\phi_1^2 - \phi_2^2}{2},$$

32

so that the first of equations (5.23) becomes

$$\frac{\phi_1^2 - \phi_2^2}{2} = (\phi_1 \phi_2 - X_0^2)\ \sinh\ (\tau_1 - \tau_2) + X_0 (\phi_1 - \phi_2)\ \cosh\ (\tau_1 - \tau_2) \quad (6.5)$$

It follows that equation (5.24) takes the form, as $X \to -\infty$,

$$\int_{\tau_2}^{\tau_1} \phi^2 d\tau = X_0^2 (\tau_1 - \tau_2) - X_0 (\phi_1 - \phi_2) + \frac{\phi_1^2 - \phi_2^2}{2} + D(N). \quad (6.6)$$

The two transcendental equations ((6.5) and (6.6)), which are independent of X, determine the limiting form of $\tau_1(X)$ and $\tau_2(X)$ on the shock wave as it travels out of the throat region. These two equations were solved numerically using a Newton-Raphson scheme in computing the results to be presented later.

Assuming that the outer limits of τ_1 and τ_2 are known from solving equations (6.5) and (6.6), it is possible to proceed with the calculation of the Fourier coefficients C_n and D_n. The procedure to be used is similar to that of Blackstock (ref. 12). Since ϕ is known explicitly as a function of τ, it is desirable to change the variable of integration in equation (6.4) to τ. In doing so, however, it must be borne in mind that the mapping from T to τ becomes discontinuous in the presence of shocks in the sense that over any period $T_2 < T < T_2 + 2\pi/\Omega$ at a given X, the values of τ range only over $\tau_1 < \tau < \tau_2 + 2\pi/\Omega$, where $\tau_2 = \tau(X, T_2)$ and $\tau_1 = \tau(X, T_1)$. The characteristics $\tau_2 < \tau < \tau_1$ can be regarded as having been "eaten up" by the shock. Thus, after shifting the integration range to $T_2 < T < T_2 + 2\pi/\Omega$, equation (6.4) can be written

$$\left\{ \begin{matrix} C_n \\ D_n \end{matrix} \right\} = \frac{\Omega}{\pi} \int_{\tau_1}^{\tau_2 + 2\pi/\Omega} (\phi^2(\tau) - X_0^2) \left\{ \begin{matrix} \cos\ n\Omega T(\tau) \\ \sin\ n\Omega T(\tau) \end{matrix} \right\} \frac{dT}{d\tau}\ d\tau$$

in which $T(\tau)$ is as given by equation (6.3). Writing the factor $\phi^2 - X_0^2$ as $(\phi + X_0)^2 - 2X_0(\phi + X_0)$, these integrals can be put in the form

$$C_n + iD_n = \frac{\Omega}{\pi} \int_{\tau_1}^{\tau_2 + 2\pi/\Omega} (\phi + X_0)^2 e^{in\Omega T(\tau)} \frac{dT}{d\tau} d\tau$$

$$-2X_0 \frac{\Omega}{\pi} \int_{\tau_1}^{\tau_2 + 2\pi/\Omega} (\phi + X_0) e^{in\Omega T(\tau)} \frac{dT}{d\tau} d\tau. \qquad (6.7)$$

The first integral in equation (6.7) becomes, after using equation (6.3),

$$\int_{\tau_1}^{\tau_2 + 2\pi/\Omega} (\phi + X_0)^2 e^{in\Omega T(\tau)} \left(1 - \frac{\phi'}{\phi + X_0}\right) d\tau, \qquad (6.8)$$

which, upon integrating the term containing ϕ' by parts, can be written

$$\int_{\tau_1}^{\tau_2 + 2\pi/\Omega} (\phi + X_0)^2 e^{in\Omega T(\tau)} d\tau + \frac{1}{2}(\phi_1 + X_0)^2 e^{in\Omega T(\tau_1)}$$

$$- \frac{1}{2}(\phi_2 + X_0)^2 e^{in\Omega T(\tau_2)} + \frac{in\Omega}{2} \int_{\tau_1}^{\tau_2 + 2\pi/\Omega} (\phi + X_0)^2 e^{in\Omega T(\tau)} \frac{dT}{d\tau} d\tau.$$

The last term of this is seen to be proportional to the original integral (6.8); thus that integral can be written, after substituting equation (6.3) for $T(\tau)$, as

$$\frac{1 + \frac{in\Omega}{2}}{1 + \frac{n^2 \Omega^2}{4}} e^{in\Omega g} I_{1n},$$

where

$$I_{1n} = \int_{\tau_1}^{\tau_2 + 2\pi/\Omega} (\phi + X_0)^\nu e^{in\Omega \tau} d\tau + \frac{1}{2} \left\{ |\phi_1 + X_0|^\nu e^{in\Omega \tau_1} - |\phi_2 + X_0|^\nu e^{in\Omega \tau_2} \right\}$$

$$(6.9)$$

34

The exponent ν in equation (6.9) is

$$\nu = 2 - in\Omega.$$

In exactly the same manner, the second integral in equation (6.7) can be shown to be

$$-\frac{(1+in\Omega)}{1+n^2\Omega^2} \ e^{in\Omega g} \ I_{2n},$$

where

$$I_{2n} = \int_{\tau_1}^{\tau_2+\frac{2\pi}{\Omega}} |\phi+X_0|^{\nu-1} e^{in\Omega\tau} d\tau$$
$$+ |\phi_1+X_0|^{\nu-1} e^{in\Omega\tau_1} - |\phi_2+X_0|^{\nu-1} e^{in\Omega\tau_2} . \qquad (6.10)$$

Finally, combining the results (6.9) and (6.10) and defining

$$J_n = |J_n| e^{-in\Omega\theta_n} = \frac{\frac{1+in\Omega}{2}}{\frac{1+n^2\Omega^2}{4}} \ I_{1n} + \frac{2X_0(1+in\Omega)}{1+n^2\Omega^2} \ I_{2n},$$

Equation (6.7) can be expressed as

$$\left\{ \begin{matrix} C_n \\ D_n \end{matrix} \right\} = \frac{\Omega}{\pi} \ |J_n| \ \left\{ \begin{matrix} \cos n\Omega(g-\theta_n) \\ \sin n\Omega(g-\theta_n) \end{matrix} \right\} \qquad (6.11)$$

It is observed that the complex J_n is independent of x; for each n it is a complex constant dependent on the paramters N, Ω, and X_0 and on the outer limit values of τ_1 and τ_2 which are known from solving equations (6.5) and (6.6). In computing the results to be discussed later, the integrals in I_{1n} and I_{2n} were evaluated numerically using Simpson's Rule for $n \geq 1$. I_{10} and I_{20} are easily evaluated analytically:

$$I_{10} = \int_{\tau_1}^{\tau_2 + 2\pi/\Omega} (\phi + X_0)^2 d\tau + \frac{1}{2} \{\phi_1^2 - \phi_2^2 + 2X_0(\phi_1 - \phi_2)\}$$

$$= \frac{\pi}{\Omega} \{N^2 + 2((1+X_0^2)^{1/2} - X_0)^2\} + 2X_0 \{(1+X_0^2)^{1/2} - X_0\}(\tau_1 - \tau_2)$$

$$+ 2X_0 N \{\sin \Omega\tau_1 - \sin \Omega\tau_2 + \frac{1}{\Omega}(\cos \Omega\tau_1 - \cos \Omega\tau_2\} - D(N),$$

$$I_{20} = \int_{\tau_1}^{\tau_2 + 2\pi/\Omega} |\phi + X_0| d\tau + (\phi_2 - \phi_1)$$

$$= -N \{(\sin \Omega\tau_1 - \sin \Omega\tau_2) + \frac{1}{\Omega}(\cos \Omega\tau_1 - \cos \Omega\tau_2)\}$$

$$+ \{(1+X_0^2)^{1/2} - X_0\}\{\frac{2\pi}{\Omega} - (\tau_1 - \tau_2)\},$$

where the shock relation (6.6) has been used in evaluating I_{10}. It is noted here that, in absence of shocks, i.e., when the inequality (5.13) is not satisfied, all of the above results which determine C_n and D_n are valid if τ_1 is simply set equal to τ_2.

The asymptotic matching of u is now completed by equating expressions (6.1) and (6.2) as required by the matching principle (ref.13). This yields the following results which determine completely the acoustic field transmitted from the throat region into x<0:

$$\delta = \epsilon^2,$$

$$A_0 = \frac{1}{2a^{1/2}} (\frac{2}{\gamma+1})^{3/2} (\frac{\omega}{2\pi a^{1/2}} |J_0| - 1),$$

$$A_n = \frac{\omega}{2\pi a} (\frac{2}{\gamma+1})^{3/2} |J_n| \quad n \geq 1, \tag{6.12}$$

$$\psi_n = \frac{\theta_n}{a^{1/2}} - \frac{1}{2a^{1/2}} \ell n \frac{2(\gamma+1)a}{\epsilon^2}.$$

The results (6.12) allow complete determination of the complex constants A_{1n} in the linear acoustic field (3.11) upstream of the throat. The constants B_{1n} are then known from equation (4.12). Several important nonlinear effects on the sound field are apparent immediately. First, the perturbation level in the outer region is an order of magnitude smaller than near the throat. This reflects the physically expected transonic trapping of the upstream propagating sound. Also, the single harmonic source at the throat generates an infinite number of harmonics in the outer region which arise, of course, because of progressive nonlinear distortion of the waveform as it moves upstream through the near-sonic flow. Finally, along with the superharmonics there is generated a steady component, or acoustic streaming term, in the outer region which is represented by the coefficient A_0 in the results (6.12).

All of the above effects have been shown previously to be present even when shock waves are not formed (ref. 5). However, the situation in which the field is continuous is likely to be exceptional in practice. The above results demonstrate that in general the acoustic field will develop shocks as the throat Mach number approaches unity. By far the major physical effect of the nonlinearity will be the dissipation of energy between the source and the exit associated with these shock waves. In order to evaluate this aspect in detail a discussion of some energy concepts will be carried out in the next chapter.

7. ENERGY CONSIDERATIONS

The existence of a shock wave in each period of the inner solution gives rise to a dissipation of fluid energy arising from viscous and heat-conduction effects modelled by the shock conditions (3.6). It is of interest to have a convenient measure of this dissipation. In linear acoustics, energy is commonly discussed in terms of the so-called acoustic energy flux, a quantity which is known to satisfy a conservation law involving only first-order acoustic quantities. The derivation of this conservation law depends upon the fact that the linear acoustic theory is a valid leading order approximation in a regular perturbation scheme about the basic state. In effect, the common acoustic energy flux vector must be the leading order approximation to some physical quantity in the exact theory. It is not immediately obvious just what this quantity is, and, more importantly, just what is its leading order approximation in a singular perturbation scheme such as that carried out in the present paper. In the following section a consistent representation of perturbation energy is suggested, although much of the lengthy detail of its development is omitted. A more complete account will appear in a later publication.

Representation of Perturbation Energy

The general energy equation for quasi-one dimensional flow can be written in terms of the present dimensionless independent variables as

$$c_s \{A(x)\bar{E}(x,t)\}_t + \{A(x)\bar{W}(x,t)\}_x = 0, \tag{7.1}$$

where $\bar{E}$ and $\bar{W}$ are the total fluid energy per unit volume (internal plus kinetic) and the total fluid energy flux, respectively; for an ideal gas

$$\bar{E} = \frac{\bar{p}}{\gamma-1} + \frac{1}{2}\bar{\rho}\bar{u}^2,$$

$$\bar{W} = \left(\frac{\bar{p}}{\gamma-1} + \frac{\bar{\rho}\bar{u}^2}{2}\right)\bar{u}. \tag{7.2}$$

Now, if the forms (3.3) are substituted into equation (7.1) and the basic steady flow equations are used as required, the energy equation becomes

$$\{c_s ARc_0^2 E^*\}_t + \{ARUc_s^2 W^*\}_t = 0$$

in which

$$E^* = \frac{p}{\gamma(\gamma-1)} + \frac{M^2}{2} \{(1+\rho)(1+u)^2-1\},$$

$$W^* = \frac{1}{(u-1)G}(p+u+pu) + \frac{M^2}{2G}\{(1+\rho)(1+u)^3-1\}.$$

Then since ARU, the mass flow rate in the basic flow, and c_s are constants, the exact energy equation in terms of the perturbations ρ, u, p can be written

$$\frac{1}{MG^{\frac{1}{2}}} E^*_t + W^*_x = 0.$$

Since, in this work, time periodic solutions ρ, u, and p are of interest it is convenient to time-average this equation over a period to obtain

$$<W^*>_x = 0 \tag{7.3}$$

in which the notation $<>$ will denote an average over a period.

The total fluid energy flux, however, is not a very useful measure of sound energy, as is well known. In particular, if the perturbation quantities are expanded according to equations (3.8) it is found that W^* contains terms of $O(\delta)$, and also that the co-efficient of δ^2 contains terms involving ρ_2, u_2, and p_2 which are not known if only the leading-order acoustic problem is solved. As was sketched in reference 1, and will be discussed in detail in a later publication, it proves to be useful to introduce a modified energy equation which is of the form

$$\frac{1}{MG^{\frac{1}{2}}} E_t + W_x = 0, \tag{7.4}$$

in which $E=E^*-\tilde{E}$, and $W=W^*-\tilde{W}$, where $\tilde{E}$ and $\tilde{W}$ can be shown to involve contributions to the total energy quantities which are not strictly attributable to the acoustic perturbation. When the modification is made, equation (7.3) is replaced by

$$I_x = <W>_x = 0 \tag{7.5}$$

where

$$W = W* - \frac{M^2}{2G}(2u+u^2) - \frac{1}{(\gamma-1)}(\rho+u+\rho u) - \frac{1}{(\gamma-1)G}(\frac{1+p}{1+\rho} -1)$$

$$= \frac{1}{(\gamma-1)G}\{pu + \frac{\rho(p-\rho)}{1+\rho}\} + \{\frac{(\gamma-1)M^2-1}{(\gamma-1)G}\}\rho u$$

$$+ \frac{M^2}{2G}\{2u^2 + \rho(3u^2+u^3)\}. \qquad (7.6)$$

The quantity W is denoted the dimensionless perturbation energy flux and is adopted as the measure of sound energy propagation. Its time-average, I, is the dimensionless average power flow per period across any station x; it is referred to as the perturbation intensity. It is emphasized that the conservation law (7.4) is an exact relation, which follows directly from the system (3.4) as can be verified by constructing suitable combinations of those three equations. No expansions of the quantities ρ, u, and p have been used in its derivation. If, however, the outer expansion (3.8) is substituted into equation (7.6) it is found that

$$W = \delta^2 W_2^{\circ} + O(\delta^4)$$

where

$$W_2^{\circ} = \frac{1}{G}(\rho_1+u_1)(\rho_1+M^2 u_1) \cong \frac{1}{G_0}(\rho_0+u_0)(\rho_0+M^2 u_0). \qquad (7.7)$$

This last expression is exactly the usual acoustic energy flux as defined, for example, by Cantrell and Hart (ref.14). Thus, the significance of W is clear: it is precisely that portion of the total energy flux in the exact theory whose leading order representation in the outer region is the common acoustic energy flux.

Physically, W can be shown to be the total fluid energy flux less a sum of terms not strictly associated with the propagation of sound. These include: (i) the energy flux in the basic steady flow, (ii) the flux of internal and kinetic energies resulting from convection of the perturbation quantities ρ, u, and p by the steady flow, and (iii) the rate of work done by the perturbation pressure against the basic flow velocity and by the basic steady pressure against the perturbation velocity. Excluding these contributions to W has the effect of removing, in equation (7.5), all of the terms in equation (7.3) which are linear in the perturbation quantities.

According to equation (7.5), the perturbation intensity I is a constant so long as shocks do not form in the field. When shocks appear then $|I|$ must decrease along the propagation direction to

account for the energy dissipated by the shocks. In the outer region the shocks become simple acoustic discontinuities; it can be shown easily that I, which in the outer region is given by $\langle W_2^o \rangle$, remains constant in the linearized theory even if these discontinuities are present.

Thus, in the event that shocks are formed in the inner region, the entire effect of these shocks on the sound energy is contained in the behavior of W in that region. The inner representation of W is complicated to derive because of the dependence on x (and thus on X and ε) of all the coefficients involving M and G in equation (7.6). In view of the fact that W is conserved in the shock-free case, it is expected that its leading order inner representation is at order ε^4 because the results (6.11) have already determined that $\delta = \varepsilon^2$. This is borne out by introducing the expansions (4.2) and (4.3) into equation (7.6) and collecting terms in the form

$$W = \sum_{m=1}^{\infty} \varepsilon^m w_m^i (X,T).$$

After considerable algebra it is found that, for the present solution in which $r_1 = -\mu_1$ and $\sigma_1 = \gamma r_1$, $w_m^i = 0$ for $m = 1,2,3$, while

$$w_4^i = \frac{2}{\gamma+1} (r_2 + \mu_2 - \mu_1^2)(r_2 + \mu_2 - 2m_1\mu_1 + \frac{\gamma-1}{2} \mu_1^2).$$

It is easily shown that the solution of equation (4.7) for $r_2 + \mu_2$ is

$$r_2 + \mu_2 = \frac{3-\gamma}{4} \mu_1^2 + m_1\mu_1 + F(T)$$

in which F(T) is an arbitrary function of T whose specific value can be determined by asymptotic matching with the outer solution but is actually unnecessary for the present purposes. Using this result and the inner solution for μ_1 puts w_4^i in the form

$$w_4^i(X,T) = \frac{2}{(\gamma+1)} F^2(T) - \frac{1}{(\gamma+1)^2} (\phi^2 - x_0^2 - 1)^2 \qquad (7.8)$$

The fact that energy flux at order ε^4 in the inner region depends on the second order inner solution r_2 and μ_2 is expected. It is known (ref. 3) that $\varepsilon^2 F(T)$ is equal to the leading order inner approximation to the downstream propagating Riemann variable for the system (3.4), which is unaffected by the nonlinearity. Hence, downstream travelling waves at order $\delta = \varepsilon^2$ in the outer region, arising from continuous reflections from the varying area, carry energy at order $\delta^2 = \varepsilon^4$ back into the inner region.

41

Sound Energy Dissipation in the Inner Region

As discussed above, the change in the sound intensity I through the inner region provides a measure of the energy dissipated by shock waves as the sound field propagates upstream. The intensity imparted to the field at the source is calculated to leading order using equation (7.8) as

$$I_s = <W_4^i(X_0,T)> = \frac{2\varepsilon^4}{\gamma+1} \{<F^2> - \frac{1}{(\gamma+1)^2} <(\phi^2-X_0^2-1)^2>_0\},$$

where the subscript 0 implies that the average is evaluated at $X=X_0$. On the other hand, the sound intensity in the outer region is represented using equation (7.7) by

$$I_{out} = \frac{\delta^2}{G_0} <(\rho_0+u_0)(\rho_0+M_0^2u_0)>,$$

which can be calculated as an infinite series of harmonics, including a steady streaming term, by use of the real parts of expressions (3.11). The difference between I_s and I_{out} is the sound power dissipated in each cycle by the shocks occurring between the source and the outer region.

Since I_{out} is a constant, and the inner and outer fields have already been matched, it follows that I_{out} must be equal to the one-term outer expansion of the one-term inner expression for I, which is

$$\lim_{X\to-\infty} \varepsilon^4<W_4^i(X,T)> = \frac{2\varepsilon^4}{\gamma+1} \{<F^2> - \frac{1}{(\gamma+1)^2} <(\phi^2-X_0^2-1)^2>_\infty\},$$

where the subscript ∞ indicates that the time average is to be evaluated in the outer limit, i.e., using equation (6.3) to relate τ to T. This determines $<F^2>$ in terms of I_{out}, and it follows that

$$\Delta I = I_s - I_{out} = \frac{2\varepsilon^4}{(\gamma+1)^3} \{<(\phi^2-X_0^2-1)^2>_\infty - <(\phi^2-X_0^2-1)^2>_0\}. \quad (7.9)$$

The required time averages in the outer limit can be calculated as in Chapter 6. For example,

$$\frac{2\pi}{\Omega} <\phi^2-X_0^2>_\infty = \int_{\tau_1}^{\tau_2+\frac{2\pi}{\Omega}} (\phi^2-X_0^2)\frac{dT}{d\tau}d\tau = \int_{\tau_1}^{\tau_2+\frac{2\pi}{\Omega}} (\phi^2-X_0^2)d\tau$$

$$+ \{\frac{\phi_1^2-\phi_2^2}{2} - X_0(\phi_1-\phi_2)\}.$$

Use of the shock condition (6.5) puts this in the form

$$\frac{2\pi}{\Omega} <\phi^2-X_0^2>_\infty = \int_0^{2\pi/\Omega} (\phi^2-X_0^2)d\tau \quad -D(N).$$

In exactly the same manner it may be shown that

$$\frac{2\pi}{\Omega} <(\phi^2-X_0^2)^2>_\infty = \int_0^{2\pi/\Omega} (\phi^2-X_0^2)^2 d\tau - \int_{\tau_2}^{\tau_1} (\phi^2-X_0^2)^2 d\tau$$

$$+ \left\{ \frac{(\phi+X_0)^4}{4} - \frac{4X_0(\phi+X_0)^3}{3} + 2X_0^2(\phi+X_0)^2 \right\} \Big|_{\tau_2}^{\tau_1}.$$

$$(7.10)$$

On the other hand, the time averages at $X=X_0$ can be evaluated with reference to figure 3 and to equation (5.25). In the range $N^*<N<N_c$, which involves two shock branches as depicted in figure 3 c and d, the integration over the period $0<T<2\pi/\Omega$ is broken into the intervals $0\leq T<\tau+$, $\tau^+\leq T<\tau_1^0$, and $\tau_1^0<T<2\pi/\Omega$. Over the first and third of these $T=\tau$, while over the middle range

$$\frac{dT}{d\tau} = 1 + \frac{2X_0\phi'(\tau)}{\phi^2(\tau)-X_0^2}$$

and τ varies over $\tau_-\geq\tau>\tau_2^0$. Hence

$$\frac{2\pi}{\Omega} < \phi^2-X_0^2>_0 = \int_0^{\tau_+} (\phi^2-X_0^2)d\tau + \int_{\tau_-}^{\tau_2^0} (\phi^2-X_0^2)d\tau + \int_{\tau_1^0}^{\tau_2^0+2\pi/\Omega} (\phi^2-X_0^2)d\tau$$

$$+ 2X_0(\phi(\tau_2^0)-\phi(\tau-)).$$

The integrals here can be combined into the form

$$\int_0^{2\pi/\Omega} (\phi^2-X_0^2)d\tau - \int_{\tau_2}^{\tau_1} (\phi^2-X_0^2)d\tau + \int_{\tau_-}^{\tau_+} (\phi^2-X_0^2)d\tau.$$

Then, use of the shock condition (5.29) with D=0 for the lower branch of the shock and of equation (6.5) for upper branch yields

$$\frac{2\pi}{\Omega} <\phi^2-X_0^2>_0 \quad \int_0^{2\pi/\Omega} (\phi^2-X_0^2)d\tau - D(N) \equiv \frac{2\pi}{\Omega} <\phi^2-X_0^2>_\infty .$$

It follows in the same manner that

$$\frac{2\pi}{\Omega} <(\phi^2-X_0^2)^2>_0 = \int_0^{2\pi/\Omega} (\phi^2-X_0^2)d\tau - \int_{\tau_2^o}^{\tau_1^o} (\phi^2-X_0^2)^2 d\tau + \int_{\tau_-}^{\tau_+} (\phi^2-X_0^2)^2 d\tau$$

$$-2X_0 \{ \frac{\phi^3}{3} - X_0^2\phi \} \Big|_{\tau_-}^{\tau_2^o} \tag{7.11}$$

Use of the above results in equation (7.9) yields for ΔI the expression

$$\Delta I = \frac{\varepsilon^4\Omega}{(\gamma+1)^3\pi} \{<(\phi^2-X_0^2)^2>_\infty - <(\phi^2-X_0^2)^2>_0\} \tag{7.12}$$

in which the averages indicated are given by equations (7.10) and (7.11). It is a simple matter to show that for N<N* equation (7.11) retains only the first term on the right side, and that for N>N_C the terms involving τ_+ and τ_- are omitted.

In every case, τ_1, τ_2, τ_1^o, τ_2^o, τ_+ and τ_- are known, and thus ΔI can be simply calculated by substituting equation (5.10) for $\phi(\tau)$. In the numerical results to be discussed later the result (7.12) was used in the form

$$\frac{I_{out}}{I_s} = \frac{1}{1+\dfrac{\Delta I}{I_{out}}}$$

to compute the fraction of power input at the source transmitted out to the duct exit.

When no shocks occur then only the first terms on the right sides of equations (7.10) and (7.11) appear. In this case, equation (7.12) yields $\Delta I=0$, which reflects the fact that sound power is conserved in the absence of shocks.

44

8. DISCUSSION OF RESULTS

The analytical results derived in the previous chapters have been evaluated numerically to study the behavior of sound transmitted upstream from an acoustic source located at the duct throat, $X_0=0$. All of the following discussion refers to a single duct geometry: the area parameter, a, was chosen to be unity, and the anechoic exit of the duct was located at $x_e=-0.5$. Of interest are the effects on the sound field of variations in the strength of the source, the fundamental frequency, and the throat Mach number. In the calculations, the acoustic power at the exit, I_{out}, was computed by the usual process of time averaging products of real parts of the complex solution given in equations (3.11) and (6.12). The input power at the source then follows from equation (7.12).

The total acoustic power I_{out} consists of a sum of terms representing the power carried in each harmonic of the outer solution. In each case these include a steady streaming component n=0. This term actually represents a modification of the basic steady flow at the level of magnitude of the perturbation field. Hence, a distinction is made in the results between the total power transmitted to the duct exit and the fluctuating power, which excludes the streaming component and is what would actually be measured as sound. It should be noted here that a significant streaming effect arises in the outer sound field because of the special choice of the source function (eq.(5.10)). Previous work in the shock-free case (ref. 4) and preliminary work in the presence of shocks indicates that when a simple harmonic source is located downstream of the throat region the streaming component developed in the field upstream is very small. Of course, in this circumstance the perturbation velocity in the throat region is markedly different from the form appearing in equation (5.10).

One other remark concerning the results is made. The dimensionless acoustic power actually calculated in the following is the actual acoustic power $ARUc_s^2<W>$ divided by a reference power corresponding to stagnation conditions, $A(0)R_sc_s^3$.

Figure 4 is included to show the typical behavior of the shock wave in the inner solution. The actual space-time path of the shock, $T=H_0(X)$, in one period is plotted over $-20 \le X \le 0$. The jump in $\epsilon\Pi$ at the shock, which is a measure of the shock strength, is also shown over the same range of X. The shock behaves in typical fashion (see ref.10): its strength grows from zero at X=0 (the source location to a maximum at $X \approx -2$, and thereafter decays monotonically as the wave travels towards the outer region.

Figures 5 and 6 illustrate the waveform of the acoustic field in the outer region for the indicated values of the parameters. The wave shapes here are determined by summing 20 harmonics in

the series (3.11) for density, ρ_0 (fig. 5), and velocity, u_0 (fig. 6). On each of the figures are shown one period of the wave at the exit location $x_e=-0.5$, and at the midpoint of the duct, $x=-0.25$. The shock wave, calculated using the results of Chapters 5 and 6 is evident as is the fact that the steady streaming effect has grown to non-negligible magnitude.

On figure 7 is shown the variation in power at the duct exit as a fraction of the total sound power introduced at the source over a range of values of the source strength parameter N. In this case shocks develop in the inner field for N>0.449. For smaller N, total power is conserved. Figure 8 displays the spreading of the total power at the exit into harmonic components. The effect of energy dissipation in the shocked inner solution is striking. From figure 7 at N=6, for example, only about 45% of the source power reaches the duct exit in the form of sound. Reference to figure 8 shows that the power carried in the fundamental harmonic at the duct exit is down to less than 30% of that introduced at the source.

Figure 9 shows the variation of the dimensionless power (referred to the reference value discussed previously) with frequency. In general it is found that dissipation increases rapidly with frequency as is seen here even for the relatively low value of N=1.5. This is expected, of course, since the higher the frequency the more shock waves occur in a given length of the duct. Figure 10 depicts the total and fluctuating power at the exit as fractions of the input power. At $\omega=5$, for example, the combination of dissipation and streaming yields a fluctuating power at the duct exit only about 20% of that at the source. It is noted, but not shown here, that only about 62% of that remains in the fundamental harmonic. It should be emphasized that the large attenuations seen in the results of figures 7-10 occur even though the throat Mach number is only 0.9. Similar results occur for even smaller Mach numbers.

Finally, figures 11 and 12 show the dependence of the outer solution on throat Mach number for fixed frequency and fixed source strength. It is noted that the effective strength of the velocity source at X=0 is εN; its value was fixed here at 0.08. Shocks occur in this case for $\varepsilon < 0.178$ or for M(0)>0.822. On figure 11 are displayed total and fluctuating power at the duct exit as fractions of the input power at the source for a frequency $\omega=2$. The marked increase in energy dissipation as the throat Mach number increases toward unity is evident. The curves on figure 12 illustrate the magnitude of the first three harmonic components of the acoustic particle velocity at the duct exit as fractions of the input velocity amplitude $\varepsilon\bar{U}$. As in the results shown in figure 9 these results verify the fact that the perturbation quantities at the exit actually approach zero as the nonlinearity becomes stronger.

46

9. CONCLUDING REMARKS

A nonlinear quasi-one dimensional theory of sound propagation through a high-subsonic throat has been developed which includes the development of shock waves in the acoustic field. The application of the theory in the present report has been to the special case in which the source of sound is located in the region where the perturbation field is essentially nonlinear. However, this case is of value in understanding the physical propagation process in that it illustrates the essential physical phenomena which occur as sound interacts with a near-sonic flow, namely the mechanism by which shocks arise and dissipate sound energy as they propagate.

Several conclusions which follow from the preceding analysis are worthy of emphasis. These are:

1. The development of shock waves is the dominant nonlinear effect associated with the interaction between sound and flow at near-sonic speeds. The shocks give rise to two kinds of physical effect on sound. First, they cause a dissipation of acoustic energy during the propagation process. Second, they can interact with a sound source located in the near-sonic region to cause an acoustic choking of the flow. In this circumstance the source can be prevented, during parts of its period, from imparting any sound energy to the flow.

2. In the present application both the nonlinear inner theory and the linearized outer theory can be solved analytically. It is found from the solution that the shock waves can undergo rather complicated motions as they traverse the near-sonic flow region.

3. The dissipation of sound energy associated with the shocks can be discussed in terms of a generalized perturbation energy flux expression developed in the report. The usual concept of acoustic energy flux is not applicable to the sound field in the region of near-sonic flow. It is found that a substantial fraction of the sound energy introduced by a source can be dissipated during the propagation process.

Current research on the nonlinear behavior of the field from a source located well outside the high-subsonic region indicates that the nonlinear effects on sound in that case are very similar to those in the present study. For example, shock waves arise in the near-sonic region in much the same way as in the present analysis, and they give rise to energy dissipation of similar magnitude. In addition, the present analytical results prove to be valuable in understanding the numerical analysis required in that case. It is hoped that they will also prove to be an aid in interpreting experimental measurements.

47

APPENDIX

The exact analytical solution for the Crocco-Tsien duct has been discussed in detail by the authors in references 1 and 5. The functions G_{in} in equation (3.11) can be taken directly from section (4.3) of reference 1 or from Appendix D of reference 5. The following parameters are defined:

$$\beta = -(\frac{\gamma+1}{2})^{\frac{1}{2}} \frac{n\omega}{K} \text{ sgn } x,$$

$$\ell = 2 + \frac{2i\beta}{\gamma+1},$$

$$\Delta = \{1 + \frac{2(\gamma-1)}{(\gamma+1)^2} \beta^2\}^{\frac{1}{2}},$$

$$j = (\ell-1-\Delta)/2, \quad k = (\ell-1+\Delta)/2,$$

in which $K^2 = 2a/(\gamma+1)$. Then, if $z = (1-K|x|)^2$,

$$G_{1n} = \{\frac{1-z}{2K}\}^{1-\ell} F(-k,-j,2-\ell;1-z)$$

$$G_{2n} = F(j,k,\ell;1-z)$$

$$G_{3n} = \{2\gamma+i\beta-(\gamma+1)\ell\}\{\frac{1-z}{2K}\}^{1-\ell} F(-k,-j,2-\ell;1-z)$$

$$G_{4n} = \frac{1}{2+i\beta} (\gamma-1+i\beta)F(j,k,\ell;1-z)$$

$$+ \frac{(\gamma+1)jk}{\ell} (1-z)F(j+1,k+1,\ell+1,1-z)$$

where $F(a_1,a_2 a_3;1-z)$ is the standard hypergeometric function with complex arguments.

The behavior of the functions G_{in}, $i=1,\ldots,4$, as $x\to 0$ also is determined in references 1 and 4. It is as given by equations (3.12) in which the constants are determined from

$$c_{12} + c_{11} = - \left\{ \frac{(\gamma+1)}{2} \, a \right\}^{\frac{1}{2}} \text{sgn } x$$

$$c_{12} - c_{11} = -(1 + \frac{in\omega}{a^{\frac{1}{2}}} \text{sgn } x) \frac{(3-\gamma)}{6} \left(\frac{2a}{\gamma+1}\right)^{\frac{1}{2}} \text{sgnx} \, ,$$

$$d\frac{+}{02} = \frac{in\omega(\gamma+1) - 2(\gamma-1) a^{\frac{1}{2}} \text{sgn } x}{in\omega(\gamma+1) - 4a^{\frac{1}{2}} \text{ sgn } x}$$

REFERENCES

1. Myers, M. K.; and Callegari, A. J.: On the Singular Behavior of Linear Acoustic Theory in Near-Sonic Duct Flows. Journal of Sound and Vibration, vol. 51, no. 4, Apr. 1977, pp. 517-531.

2. Callegari, A. J.; and Myers, M. K.: Nonlinear Effects on Sound in Nearly Sonic Duct Flows. AIAA Paper No. 77-1296, Oct. 1977.

3. Myers, M. K.; and Callegari, A. J.: Transmission of Sound Through High-Subsonic Flows in Non-Uniform Ducts. AIAA Paper No. 78-1155, July 1978.

4. Callegari, A. J.; and Myers, M. K.: Sound Transmission in Ducts Containing Nearly Choked Flows. AIAA Paper No. 79-0623, March 1979.

5. Callegari, A. J.: Nonlinear Effects on Sound Propagation Through High Subsonic Mach Number Flows in Variable Area Ducts. NASA CR-3138, May 1979.

6. Myers, M. K.; and Callegari, A. J.: Acoustic Shocks in Nearly Choked Duct Flows. AIAA Paper No. 80-1019, June 1980.

7. Nayfeh, A. H.; Shaker, B. S.; and Kaiser, J. E.: Computation of Nonlinear One Dimensional Waves in Near Sonic Flows. AIAA Journal, vol. 16, Nov. 1978, pp. 1154-1159.

8. Nayfeh, A. H.; Kelley, J. J.; and Watson, L. T.: Nonlinear Propagation in Near Sonic Flows. Journal of Sound and Vibration, vol. 75, no. 3, Apr. 1981, pp. 359-370.

9. Liepmann, H.; and Roshko, A.: Elements of Gasdynamics. New York, John Wiley and Sons, 1957.

10. Whitham, G. B.: Linear and Nonlinear Waves. New York, John Wiley and Sons, 1974.

11. Courant, R.; and Hilbert, D.: Methods of Mathematical Physics, Vol. II. New York, Interscience, 1962, Chapter II.

12. Blackstock, D. T.: Connection Between the Fay and Fubini Solutions for Plane Sound Waves of Finite Amplitude. Journal of the Acoustical Society of America, vol. 39, 1966, pp. 1019-1026.

13. Van Dyke, M.: Perturbation Methods in Fluid Mechanics.
    Annotated Edition. Stanford, Parabolic Press, 1975.

14. Cantrell, R. H.; and Hart, R. W.: Interaction Between Sound
    and Flow in Acoustic Cavities: Mass, Momentum, and Energy
    Considerations. Journal of the Acoustical Society of
    America, vol. 36, 1964, pp. 697-706.
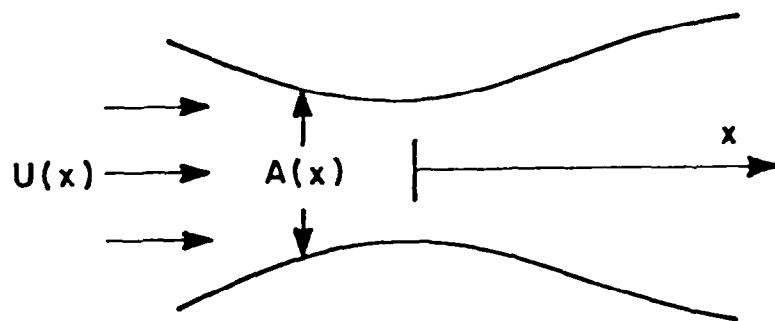
Figure 1.-Typical duct geometry.
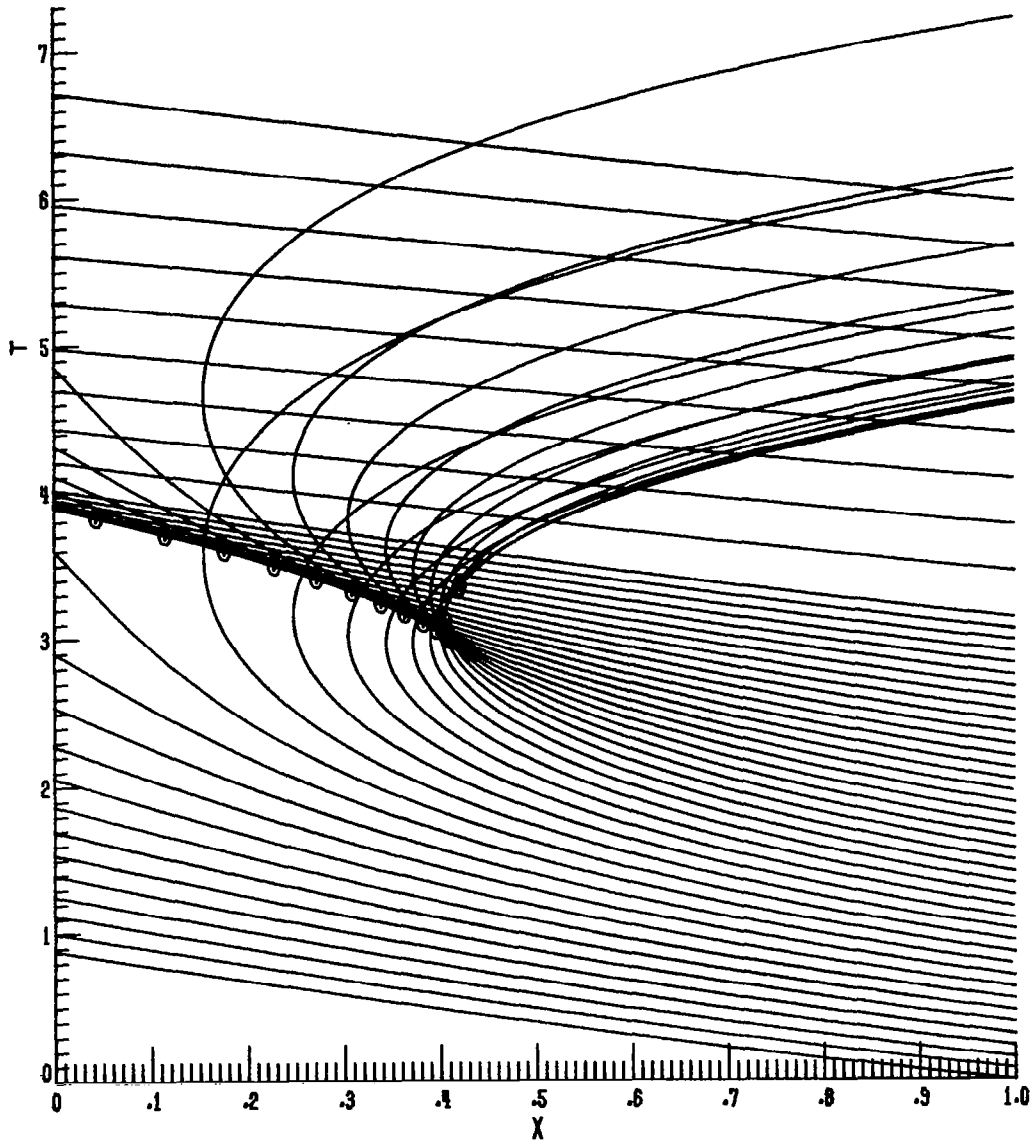
(a) N=0.5.

Figure 2.-Characteristic curves over one period
$0 \leq \tau < 2\pi/\Omega$; $X_0 = \Omega = 1$.
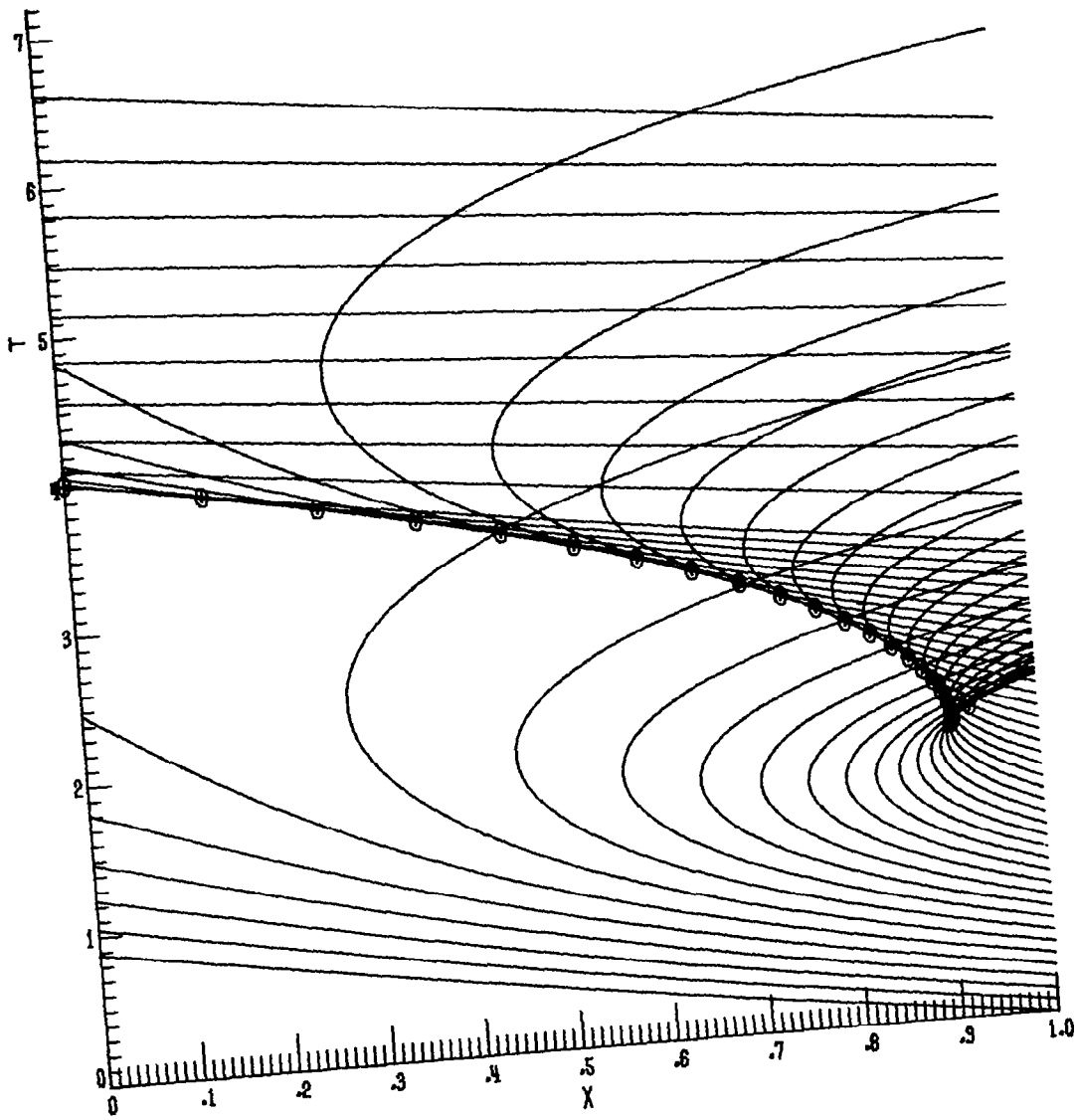
(b) N=1.0.

Figure 2.-Continued.

54
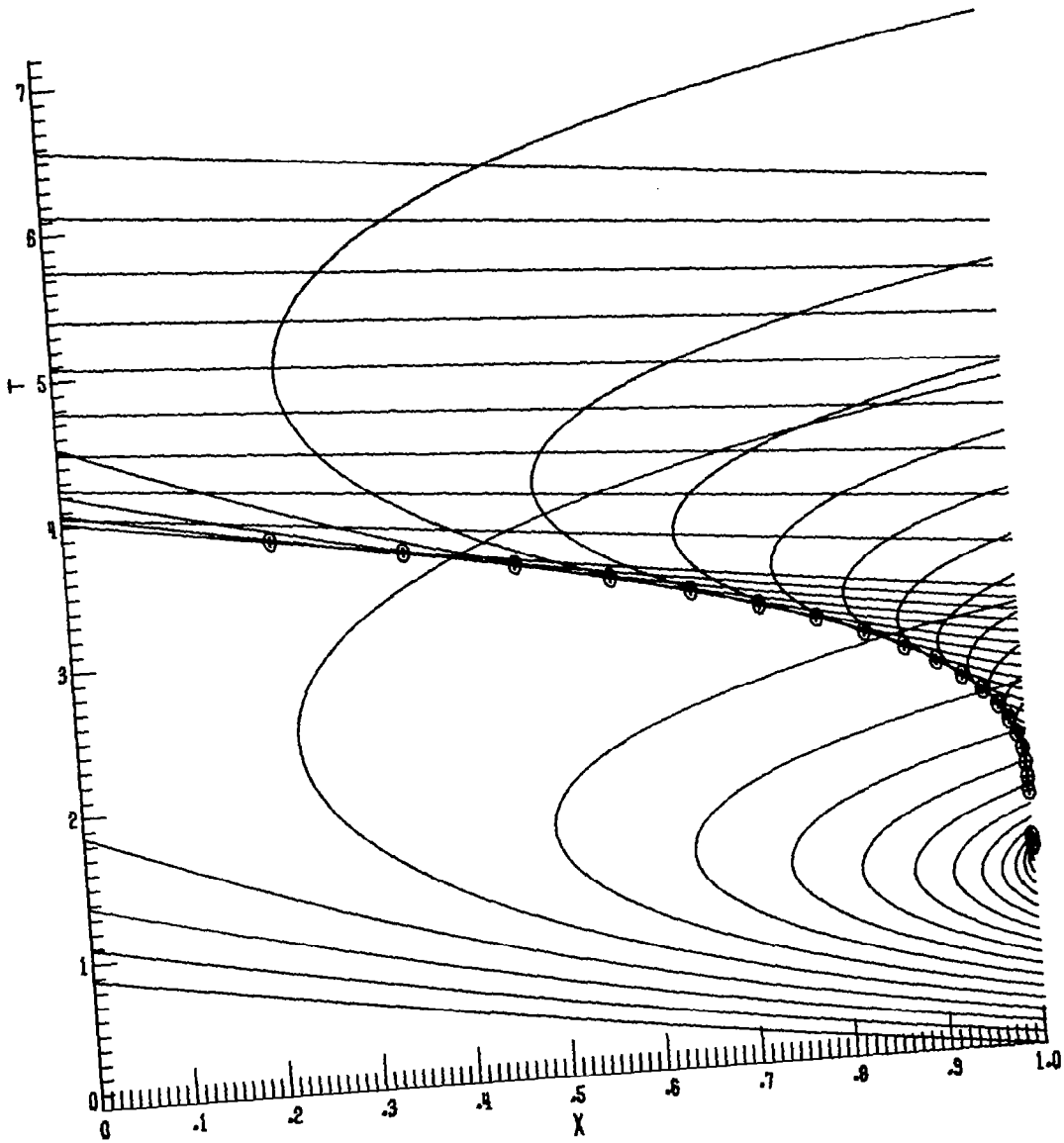
(c) N=1.432.

Figure 2.-Continued.
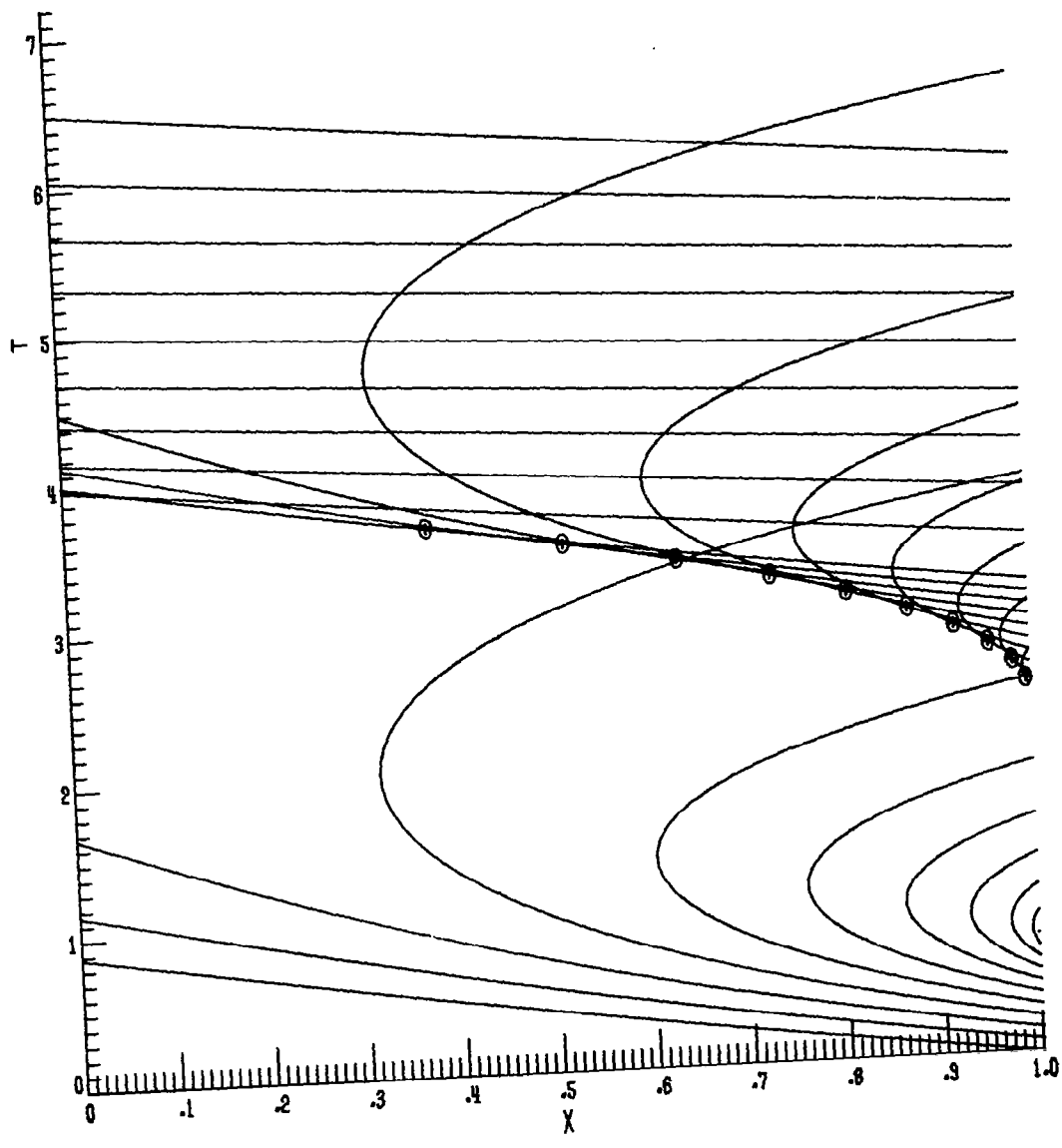
(d) N=1.60.

Figure 2.-Concluded.
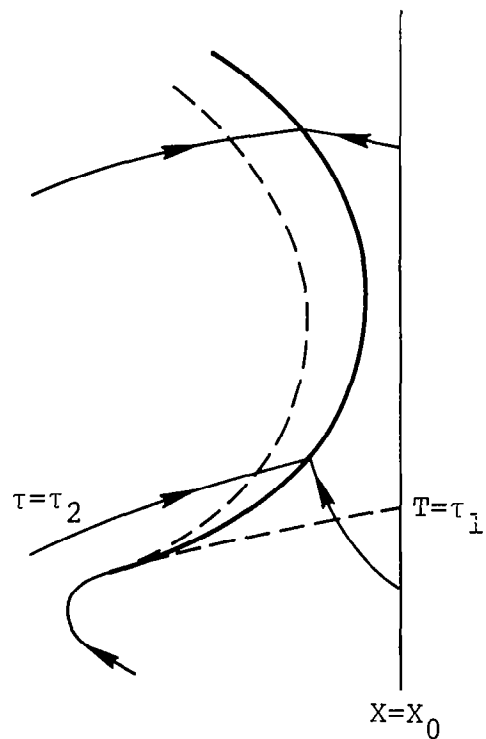
(a) $N<N^*$.
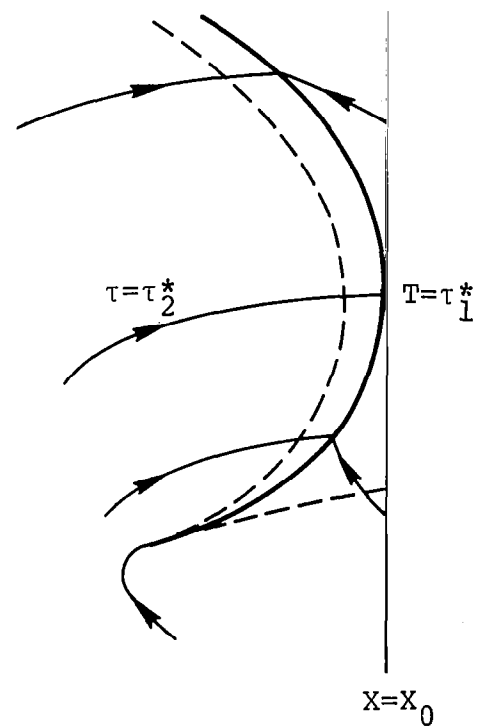
(b) $N=N^* \ (1+X_0^2)^{\frac{1}{2}}$.

Figure 3.-Schematic representation of characteristics
and shock near $X=X_0$.
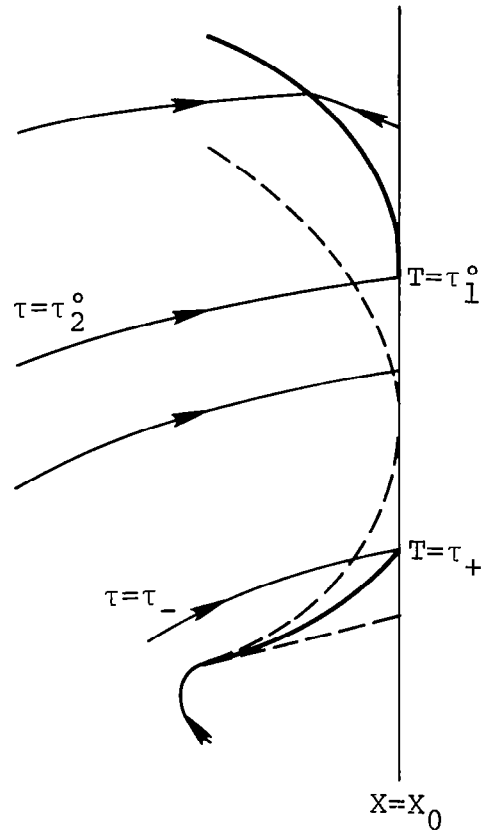
(c) $N=(1+X_0{}^2)^{1/2}$.
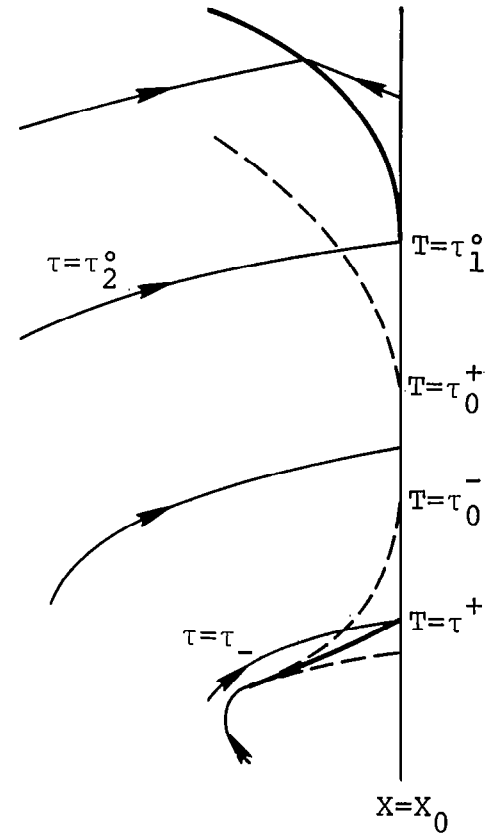
(d) $(1+X_0{}^2)^{1/2}<N<N_c$.

Figure 3.-Concluded.
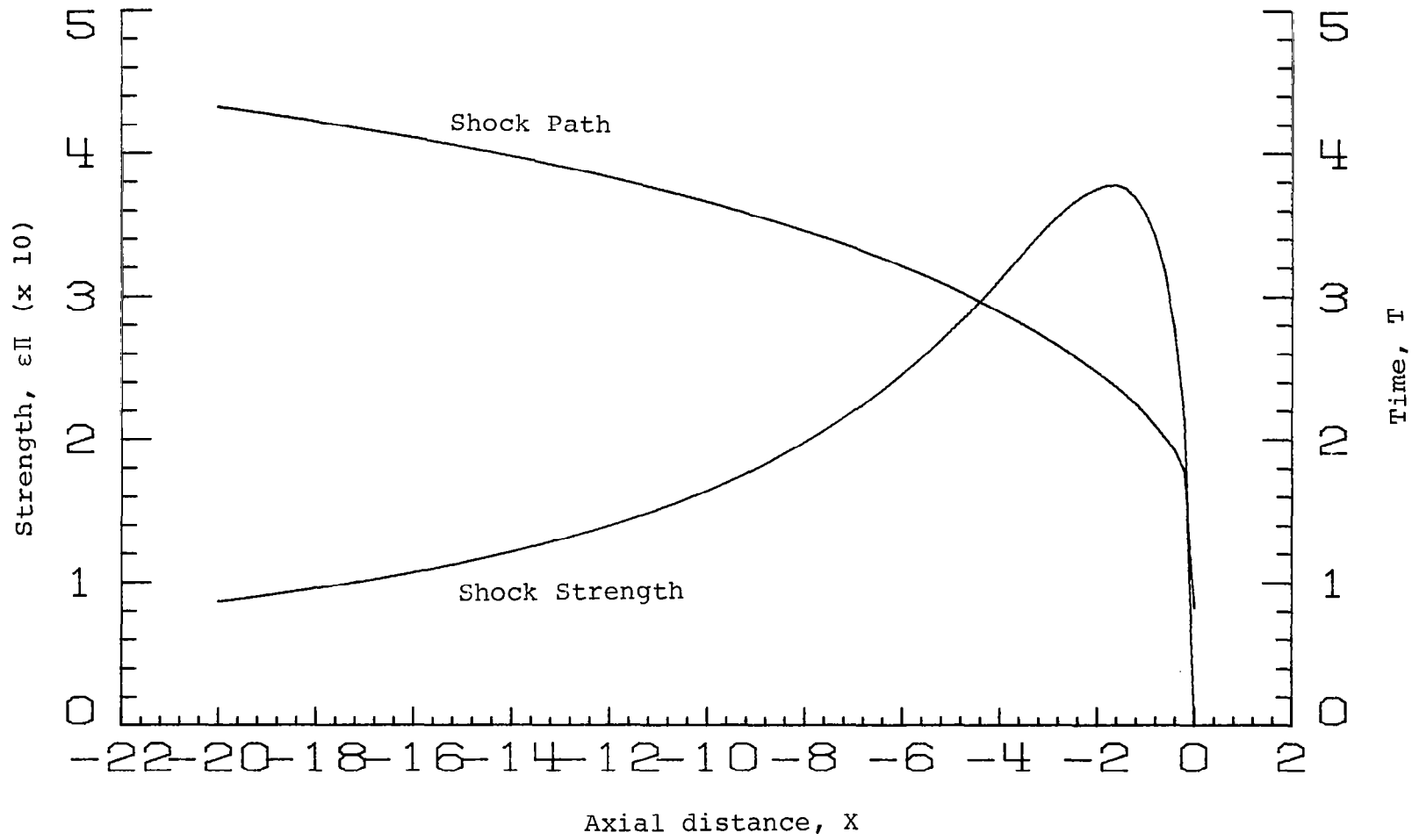
Figure 4.-Shock strength and path: N=5, ε=0.1, ω=2.
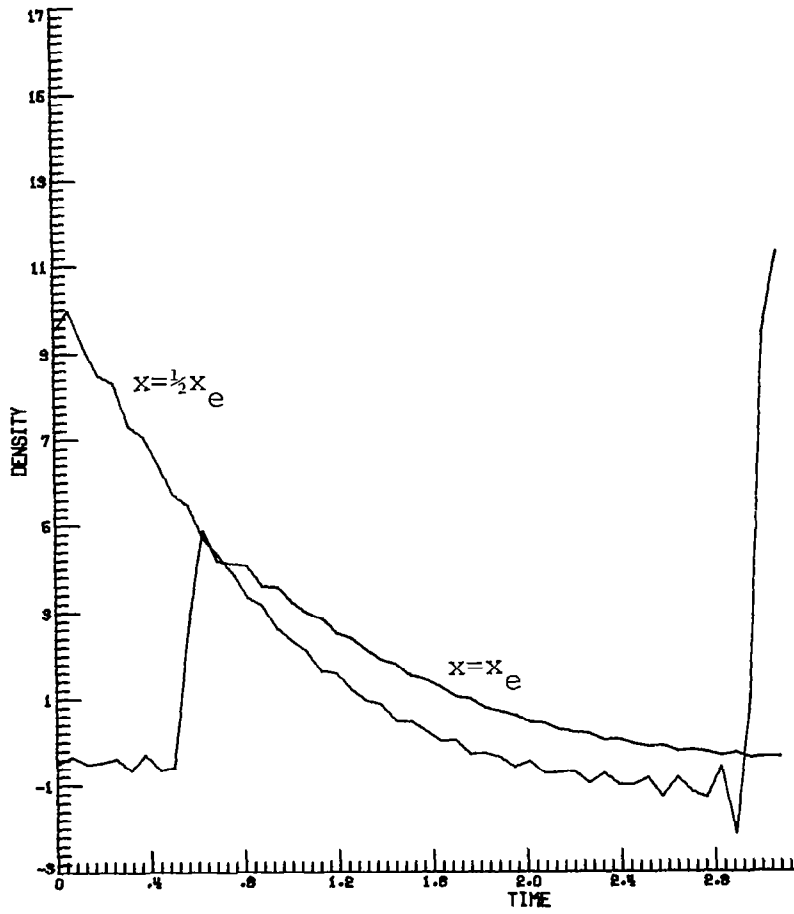
Figure 5.-Time history of perturbation density ρ_0: N=2, ω=2, ε=0.1, x_e=0.5, 20 harmonics.
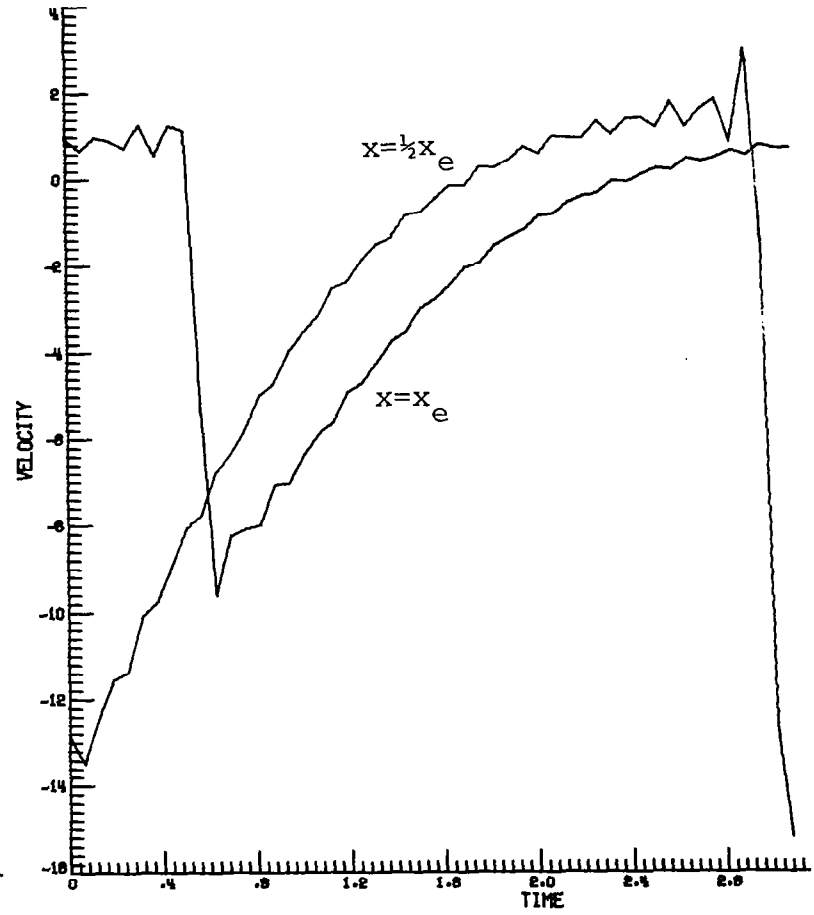
Figure 6.-Time history of perturbation velocity u_0: N=2, ω=2, ε=0.1, x_e=0.5, 20 harmonics.
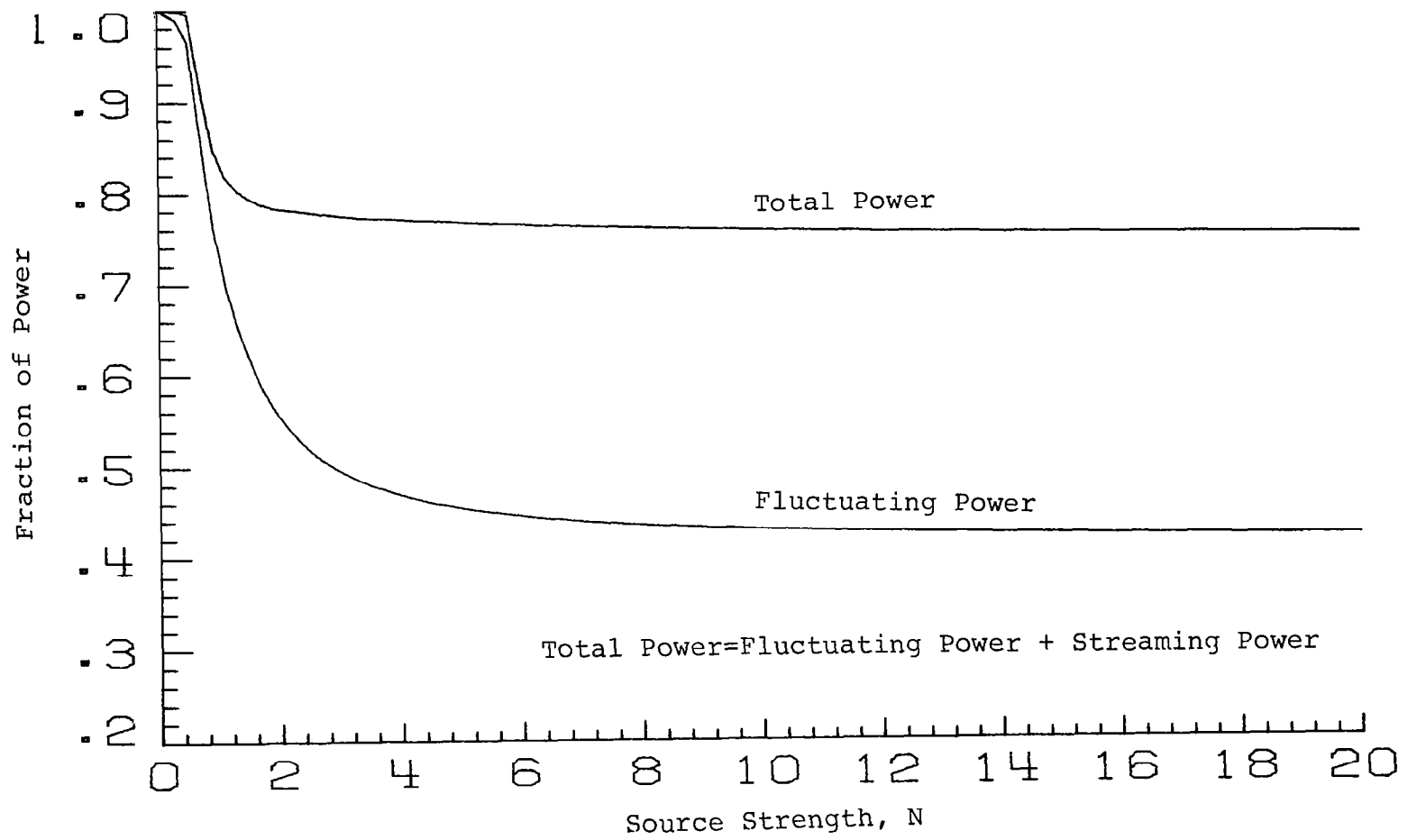
Figure 7.-Fraction of input power reaching exit
vs. source strength: ε=0.1, ω=2.
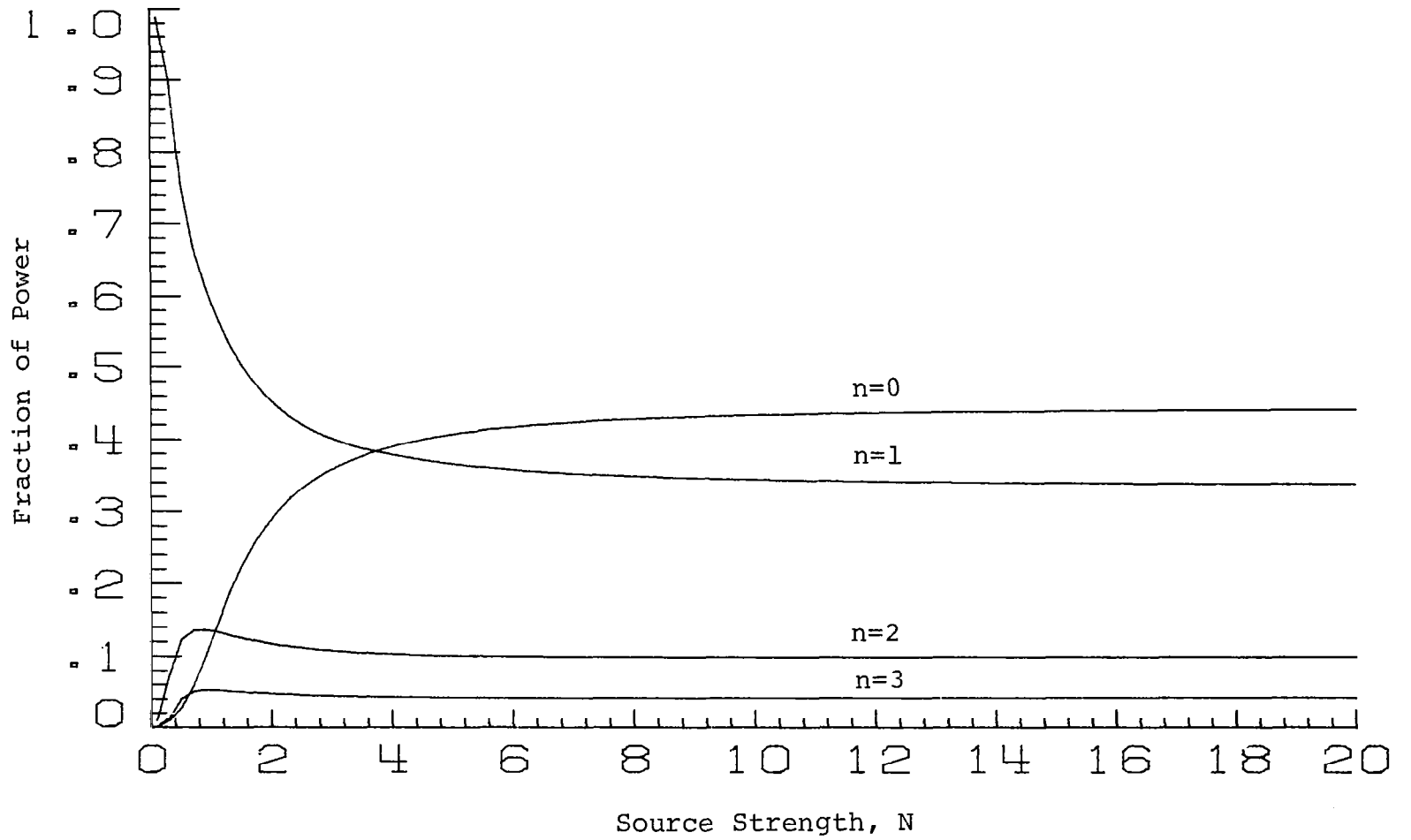
Figure 8.-Fraction of total power at exit in harmonics
vs. source strength: $\varepsilon=0.1$, $\omega=2$.
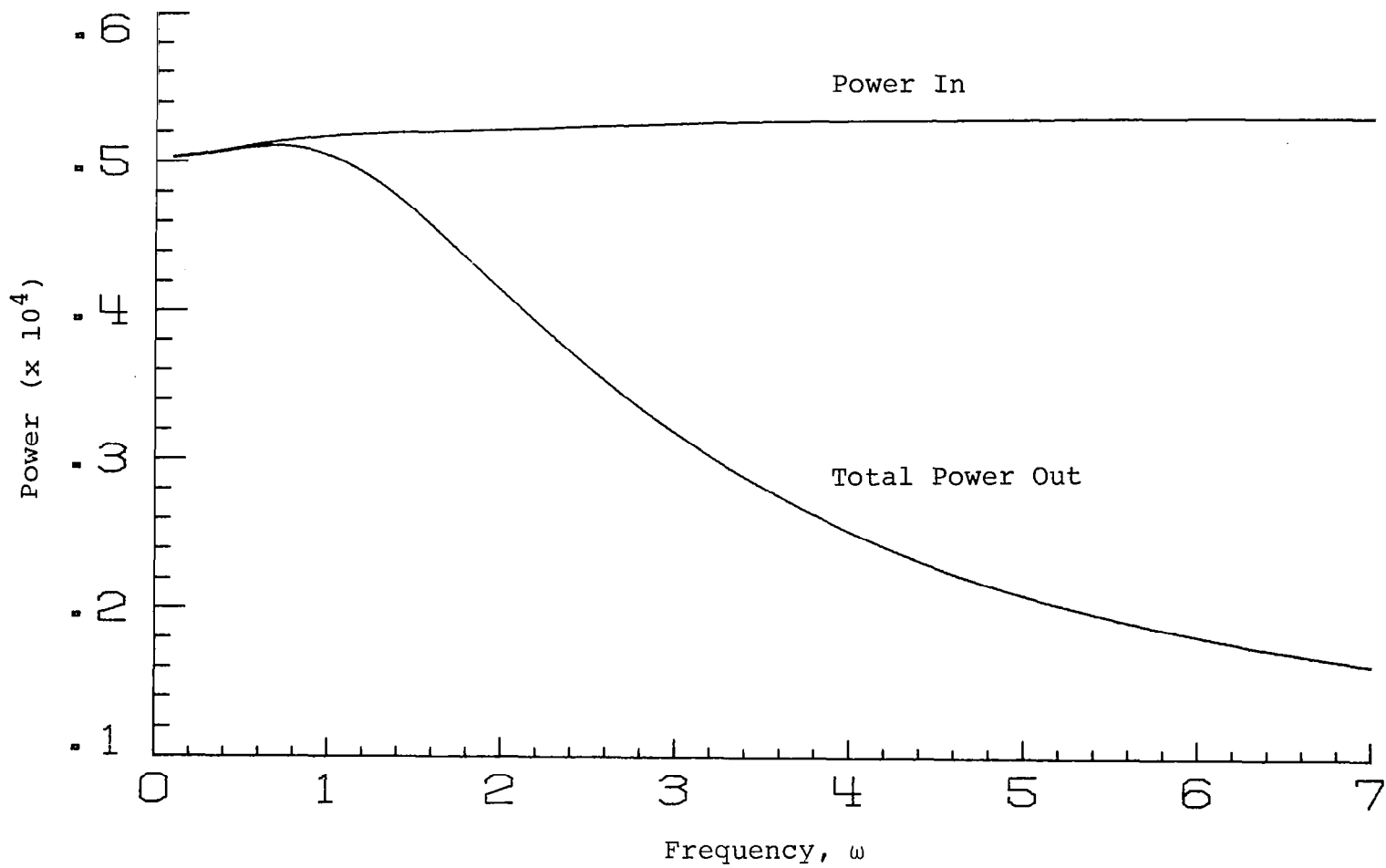
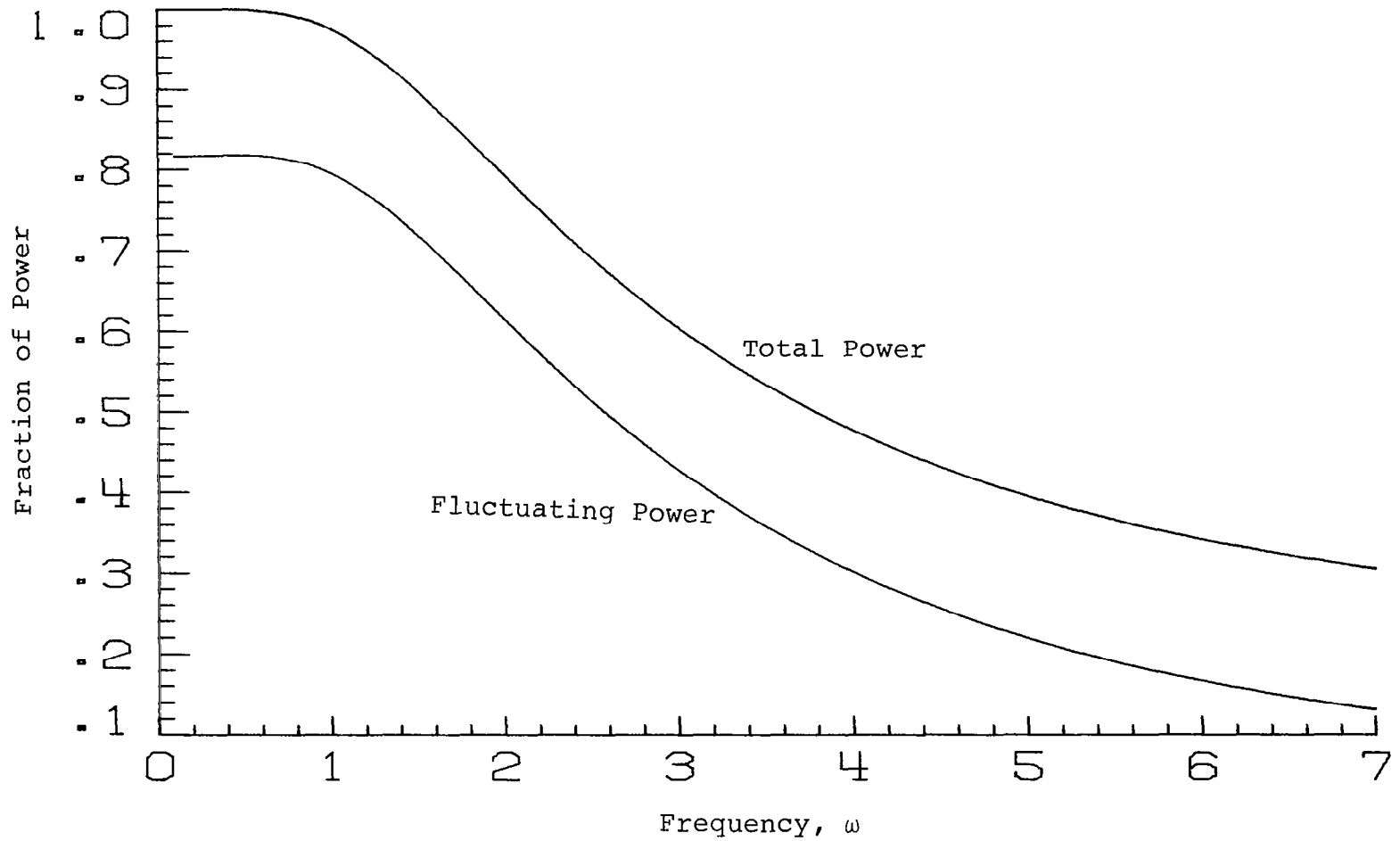Figure 9.-Total power in at source and out at exit
vs. frequency: ε=0.1, N=1.5.

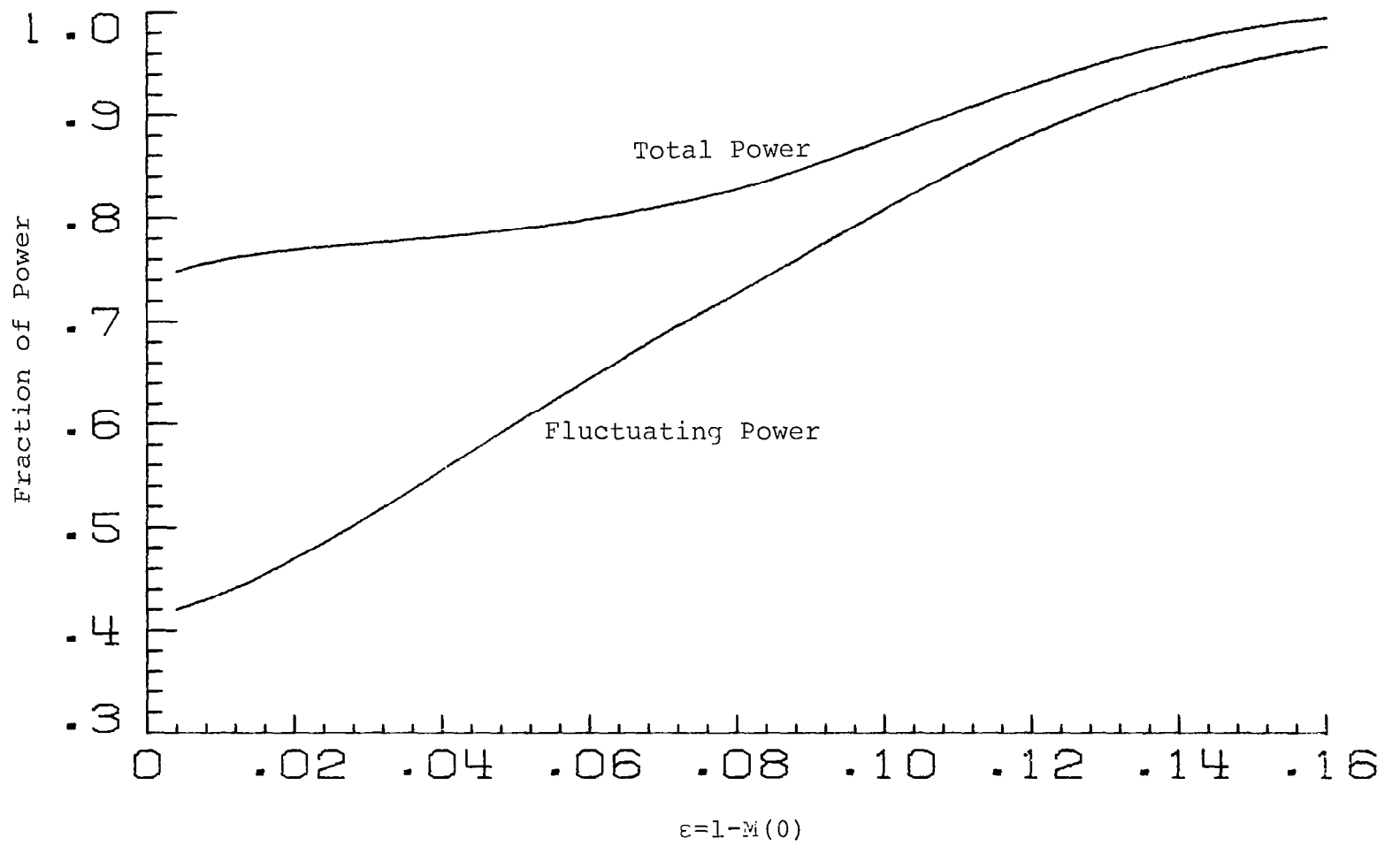Figure 10.-Fraction of input power reaching exit
vs. frequency: ε=0.1, N=1.5.

Figure 11.-Fraction of input power reaching exit
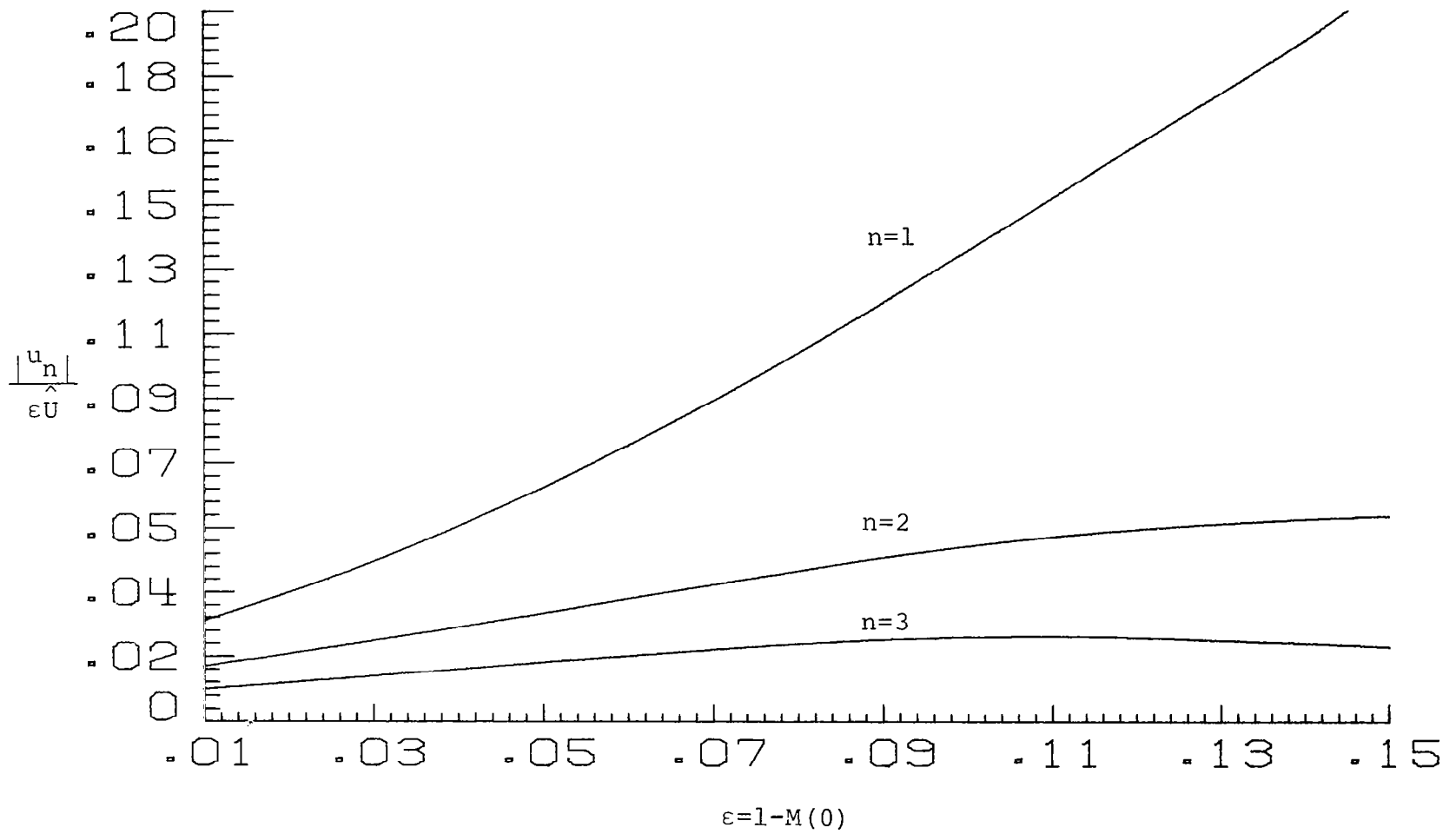vs. throat Mach number: $\varepsilon N=0.08$, $\omega=2$.

Figure 12.-Acoustic velocity at exit vs. throat
Mach number: $\varepsilon N=0.08$, $\omega=1$.